Addressing the Challenges of the Design of Hypersonic Vehicles with Simulation

Swati Saxena, PhD

January 23, 2021

Presented at AIAA LA-LV Section

Contributors:

Valerio Viti, PhD

Craig Miller, PhD

Scott Marinus

Bruce Crawford

Jeff Tharp, PhD

Walt Schwarz, PhD

Eldon Staggs

Ansys

Ansys Offers the True Simulation Platform

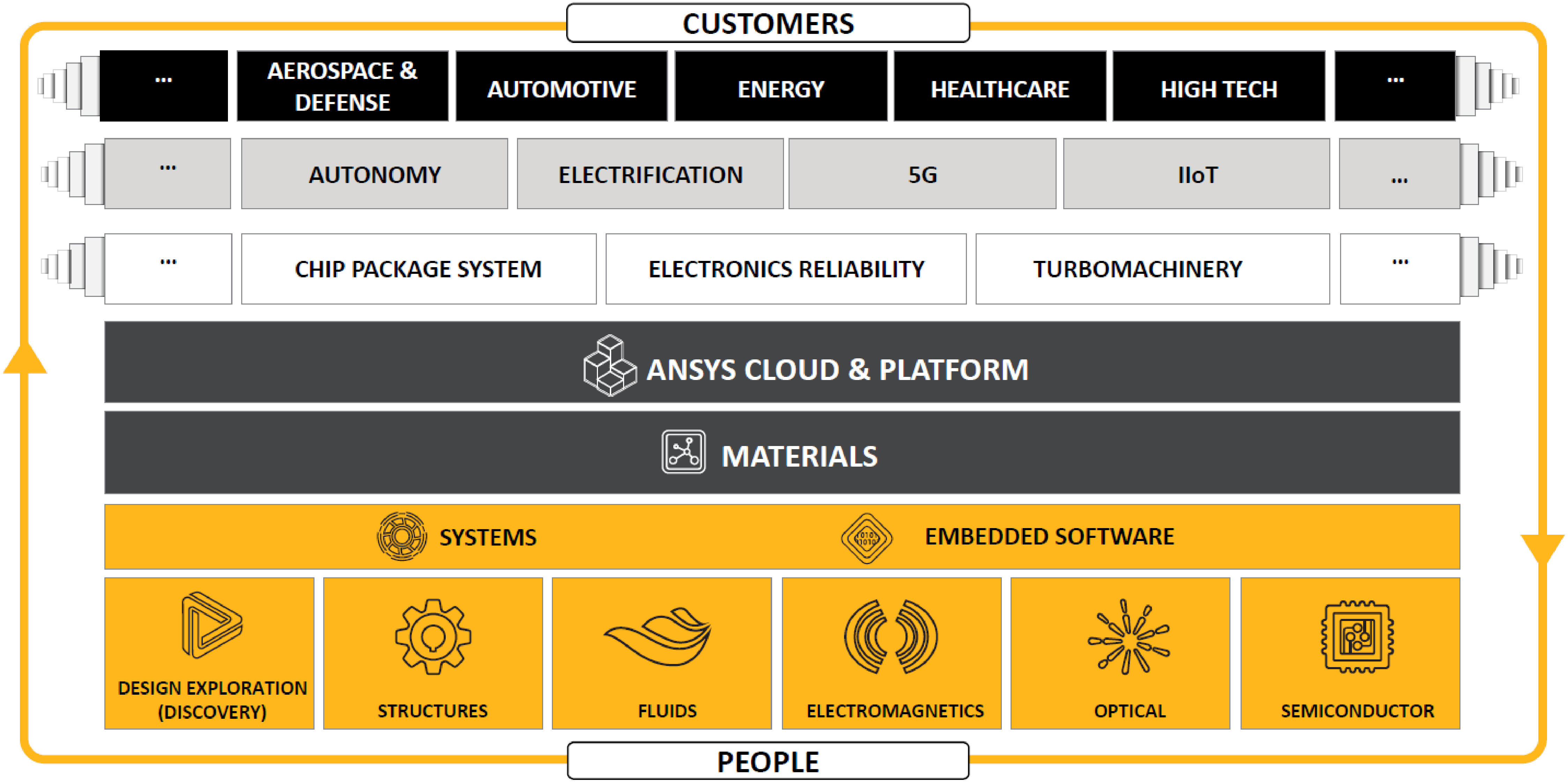

Outline

- Hypersonics - Introduction
- Overview of the Ansys solutions for hypersonics
- Use Cases:
  - Aerodynamics: Aerospiked Missile, Sphere and Scramjet
  - Fluid-Structural Interaction: Projectile at Mach 10
  - Communication Blackout: Biconic with flaps, hyperboloid re-entry capsule
  - Mission Planning
- Ansys Advantage
  - Ansys R&D and collaboration with select Universities
  - Training and validations

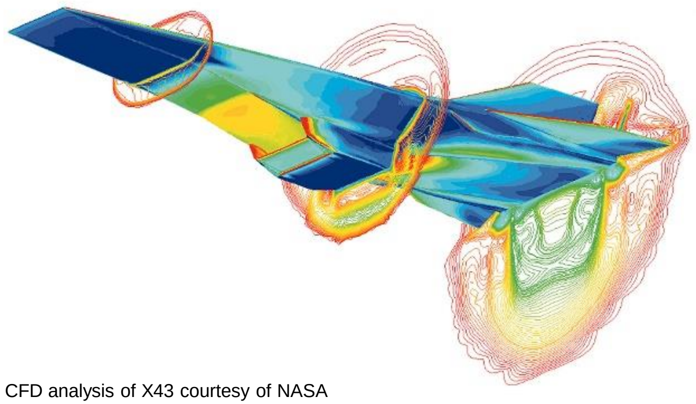

CFD analysis of X43 courtesy of NASA

Hypersonic Vehicle - Introduction

- ## Why now?

More recently, the US Department of Defense (DoD) has been actively pursuing and supporting the development of hypersonic weapons and vehicles owing to the continued threat from adversaries.

The Pentagon's FY2021 budget request for all hypersonic related research is at $3.2B[1] – up from $2.6B in FY2020.

- ## Operational advantage

Systems that operate at hypersonic speeds— offer potential for military operations from longer ranges with shorter response times and enhanced effectiveness compared to current military systems. Also, commercial aviation hypersonic applications would connect various parts of the world faster.

> *"U.S. officials have referred to hypersonic weapons as their "first, second, and third" weapons development priorities"*
> The Washington Post

Hypersonic vehicle design challenges

Design of Hypersonic vehicles extremely challenging

- Hypersonic vehicle flies for part of its trajectory at Mach number above 5 (speed of sound is Mach 1 at 343 m/s at STP).
- These extreme operational conditions pose unique challenges in the design, manufacturing, and sustainment of these vehicles.
- The development of hypersonic systems has several technical challenges which must be addressed due to the severity of flight operating conditions and requirements:
  - Propulsion systems, aerothermodynamics, & airframe/propulsion integration
  - Material selection, structural design, and thermal protection systems
  - Navigation, guidance, & control to name a few

Hypersonic Technology Vehicle-2.
Source: DARPA

Why Simulation is important?

- Very difficult to create real flight conditions and environment during physical tests.
- Physical testing is very expensive and extremely time consuming. It limits design evaluation space.
- Virtual prototyping is the solution: Multiphysics simulation platforms with HPC can now accurately capture these physical phenomena, produce reliable results and simulate real flight conditions over the entire design space to accelerate design cycle.

Hypersonic vehicle design is rocket science…

- How to get there
  - Propulsion
  - Aerothermodynamics
- How to survive
  - Structural integrity
  - Materials
- How to control the vehicle
  - Flight control system
  - Sensors
  - Communication and tracking
- Everything must work closely together
  - System integration and embedded software
  - Strong coupling between different physics

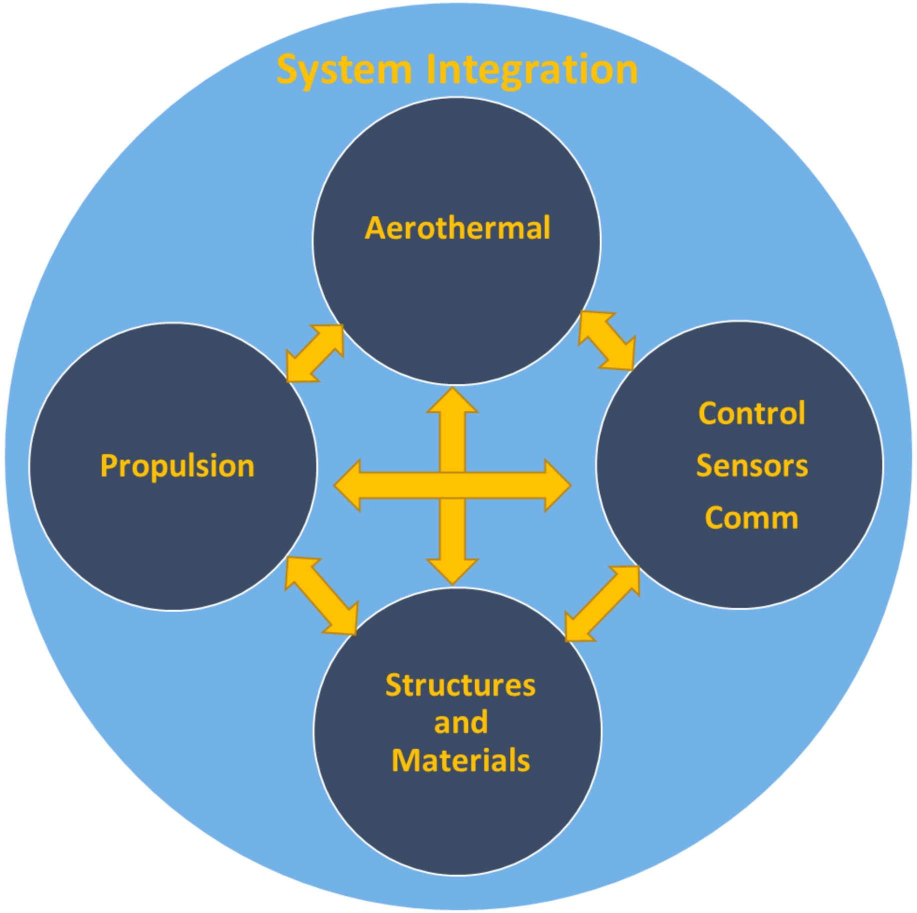

Simulation Needs for Hypersonic Vehicles

Platform and workflow
- Platform agnostic
- Data and process management
- Traceability

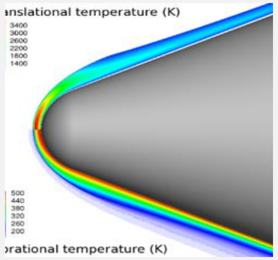

Aerothermodynamics
- Heat fluxes and aero forces
- Shock location and behavior
- Laminar-Turbulent transition
- Flow control
- Chemical non-equilibrium
- Thermodynamic non-equilibrium
- Ablation

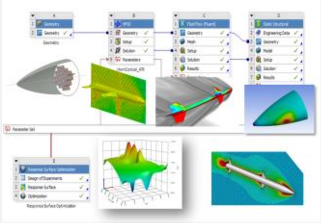

Process Integration and Design Optimization
- Platform agnostic
- Multiphysics
- Parametric analysis
- Design optimization
- Data and process management
- Traceability

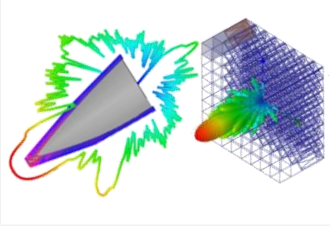

Communication and tracking
- Antennas and sensors
- Radio/GPS jamming
- Radar/IR signature
- Structural deformation
- Vibration impact
- Communication black-out

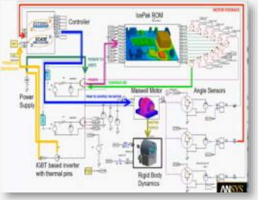

System integration
- Control system integration
- Sensor fusion and actuation
- Navigation, guidance and control
- “Wargaming” and mission-level simulation

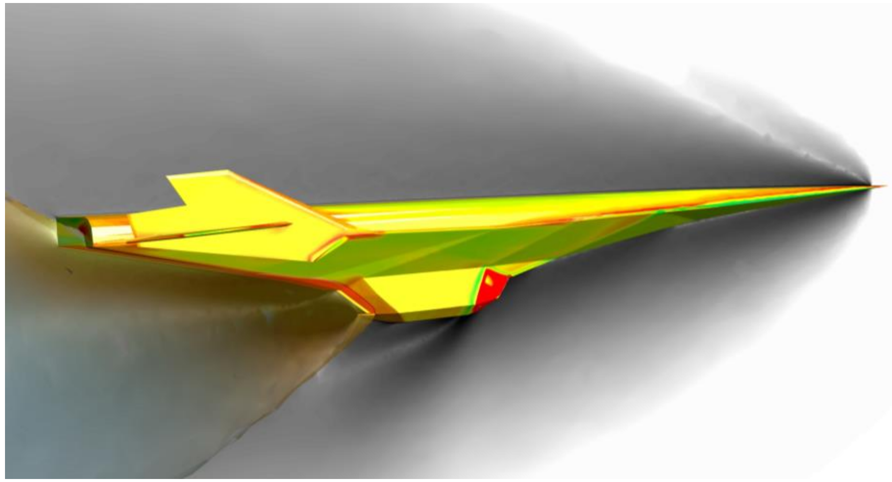

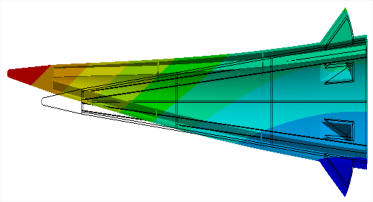

Structure and materials
- FSI/Deformation
- Fracture and fatigue
- Structural integrity
- Material intelligence

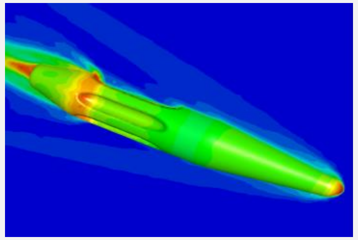

Thermal management
- Radiation, Conv., Cond.
- Conjugate Heat Transfer
- Active cooling
- Phase change: boiling, evapor./condensation
- Melting/solidification
- Electronics cooling

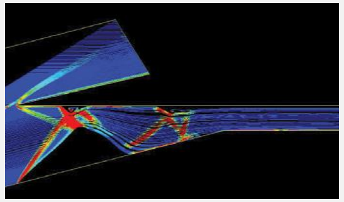

Propulsion
- RAM/SCRAMJET combustion
- Solid/Liquid rocket
- Gas, liquid and solid fuels
- Thermal loads
- Structural deformation

Prototype based on original published work at Sandia by Jordan, *“Jordan, T.M., Buffington, R.J., Aerodynamic Model for a Hemispherically-Capped Biconic Reentry Vehicle with Six Drag Flaps. AIAA Paper 87-2364, 1987.”*

Ansys

Ansys Hypersonics Solution Overview and Readiness

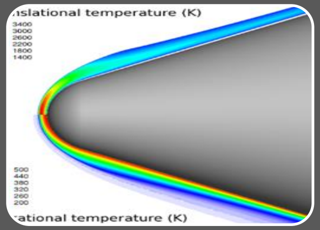

Aerothermodynamics
- Heat fluxes and aero forces
- Shock location and behavior
- Laminar-Turbulent transition
- Flow control
- Chemical non-equilibrium
- Thermodynamic non-equilibrium
- Ablation

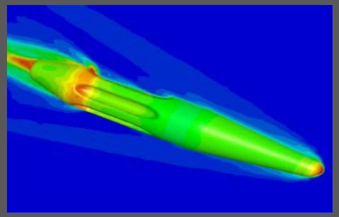

Thermal management
- Radiation, Convection, Conduction
- Conjugate Heat Transfer
- Active cooling
- Phase change: boiling, evapor./condensation
- Melting/solidification
- Electronics cooling
- Sensor thermal cycling

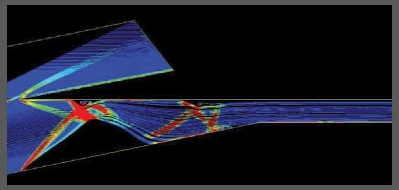

Propulsion
- RAM/SCRAMJET combustion
- Gaseous, liquid and solid fuels
- Thermal loads
- Structural deformation
- Inlet/nozzle performance

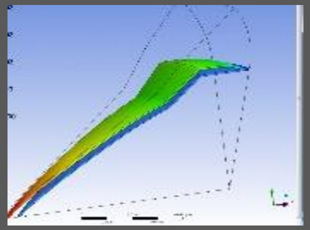

Structure and materials
- FSI/Deformation:
  - steady-state
  - transient
- Fracture and fatigue
- Structural integrity
- Material intelligence

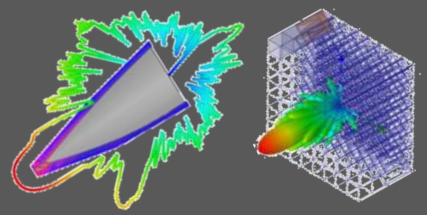

Communication and tracking
- Antennas and sensors
- Radio/GPS jamming
- Radar/IR signature
- Structural deformation/vibration impact
- Communication black-out
- Sensor reliability

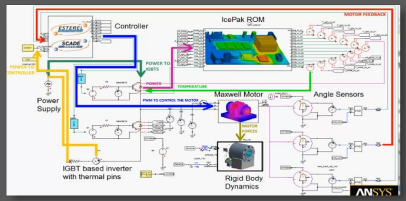

System integration
- Control system integration
- Sensor reliability and fusion
- Navigation, guidance and control
- "Wargaming" with 3rd party integration

Platform and workflow
- Platform agnostic
- Data and process management
- Traceability

Ansys Technology Stack for Hypersonics

Aerodynamics	Propulsion	Materials & Structures	Communication & Tracking	System Integration

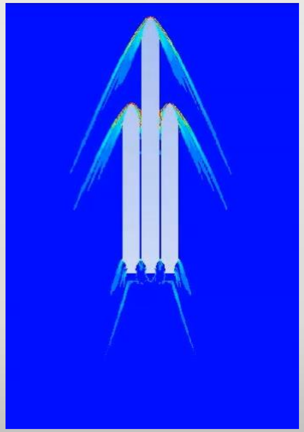

Aircraft/booster Separation

- Trajectory computation
- Aerodynamic interference
- Shock impingement

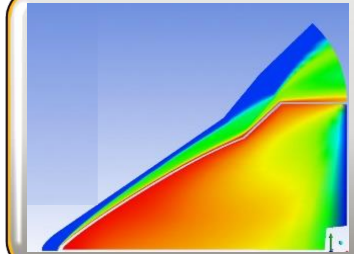

Aerothermodynamics

- Shock capturing and location
- Pressure distribution
- Skin friction, Wall heat flux
- Inlet conditions for engines
- Turbulence transition
- Flow control

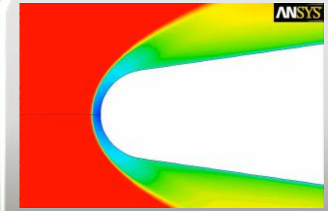

Ablation

- Surface finite-rate reactions
- Charring and erosion
- Surface recession
- LE/Nose/flap shape change

Hypersonic Technology Vehicle-2.
Source: DARPA

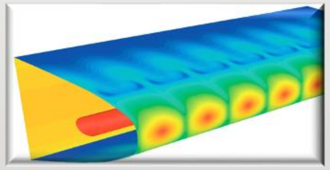

Active cooling

- Single/Multi-phase
- Radiation, Convection, Cond
- Phase change: boiling, evaporation/condensation
- Jet impingement

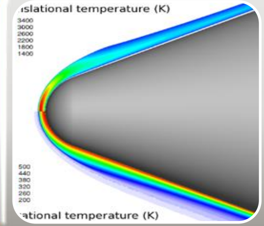

Chemical non-equilibrium

- Species transport, finite-rate reactions
- Dissociation, ionization, recombination
- Equilibrium and non-equilibrium
- Flexible and powerful chemical solver

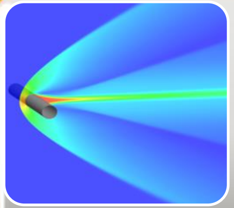

Plasma activation

- Ion concentration
- Lorentz forces
- Communication blackout

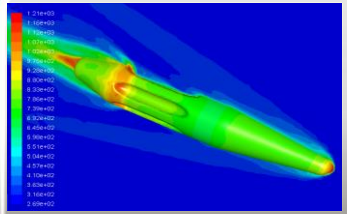

Conjugate HT

- Radiation, Convection, Cond
- Surface and structure conduction
- Melting/solidification

Ansys

Ansys Hypersonics Aerodynamics Validation Cases

Re-entry capsule with counter-flowing jet, Mach 3.5, Turbulent, Air as ideal-gas (Daso case)

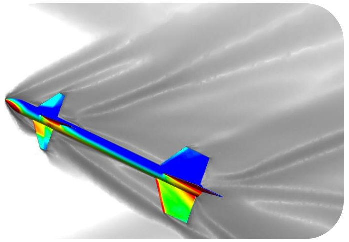

NASA TCM, Mach 3.5, Turbulent, Air as ideal-gas

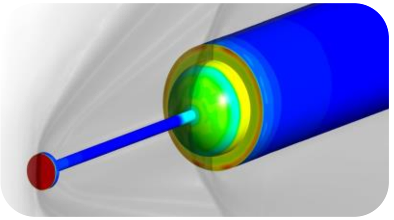

Aerospike at Mach 6, Turbulent, ideal gas

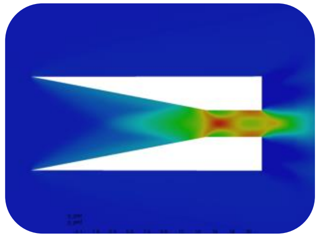

Kussoy Hypersonic inlet at Mach 8.3, Turbulent, air as ideal-gas

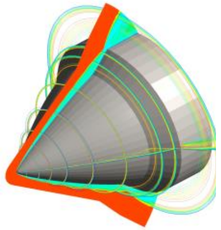

Hyperboloid, Mach 9.85, laminar, Chemical non-equilibrium (Park II)

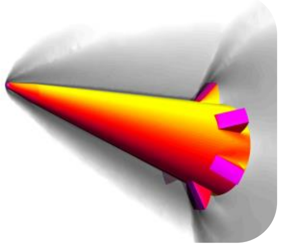

Biconic with flaps at Mach 10.3, Turbulent, N_2 as ideal-gas

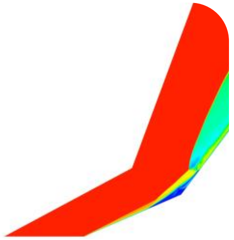

Double cone at Mach 12.6, Laminar, Thermodynamic non-equilibrium

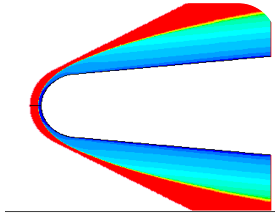

Blunt-cone at Mach 25, Laminar, Chemical non-equilibrium

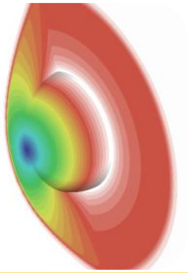

Sphere at Mach 29, Laminar, Chemical non-equilibrium

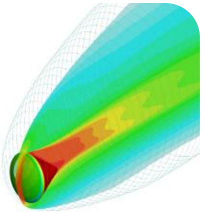

FIRE II, Re-entry capsule, Turbulent, Mach 35.7, Air in chemical non-equilibrium (Gupta)

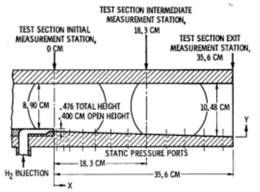

Burrow's SCRAMJET, Mach 2.44, Turbulent, H_2

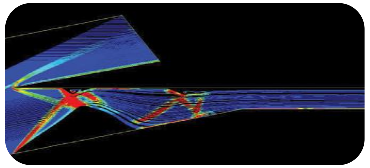

Bapu's SCRAMJET at Mach 3.45, Turbulent, Hydrocarbon

Ansys Hypersonics Aerodynamics Validation Cases

Re-entry capsule with counter-flowing jet, Mach 3.5, Turbulent, Air as ideal-gas (Daso case)

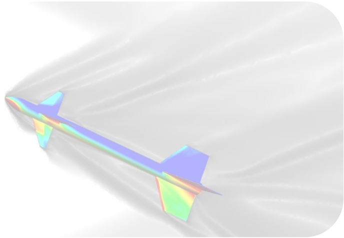

NASA TCM, Mach 3.5, Turbulent, Air as ideal-gas

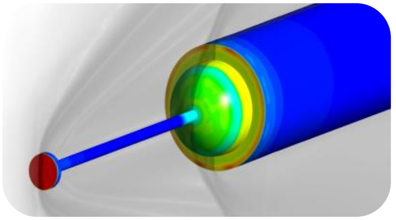

Aerospike at Mach 6, Turbulent, ideal gas

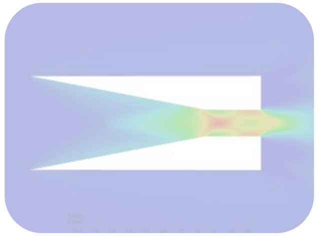

Kussoy Hypersonic inlet at Mach 8.3, Turbulent, air as ideal-gas

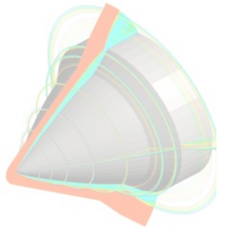

Hyperboloid, Mach 9.85, laminar, Chemical non-equilibrium (Park II)

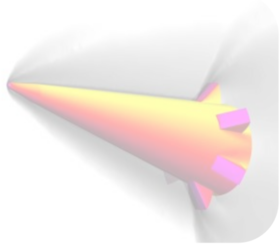

Biconic with flaps at Mach 10.3, Turbulent, N_2 as ideal-gas

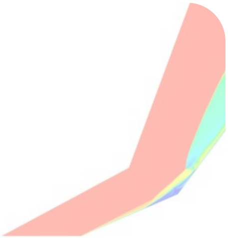

Double cone at Mach 12.6, Laminar, Thermodynamic non-equilibrium

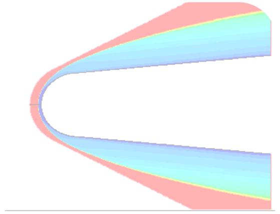

Blunt-cone at Mach 25, Laminar, Chemical non-equilibrium

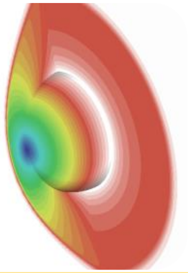

Sphere at Mach 29, Laminar, Chemical non-equilibrium

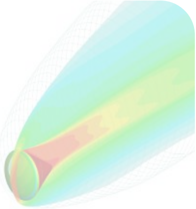

FIRE II, Re-entry capsule, Turbulent, Mach 35.7, Air in chemical non-equilibrium (Gupta)

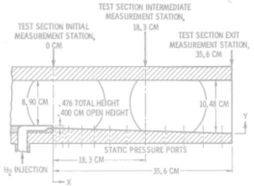

Burrow's SCRAMJET, Mach 2.44, Turbulent, H_2

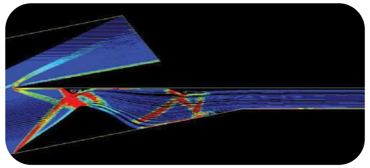

Bapu's SCRAMJET at Mach 3.45, Turbulent, Hydrocarbon

Ansys

Case study 1: Validation of Aerospiked Missile at Mach 6

Work based on an aerospike geometry with and aerodisk proposed by Hubner et Al. at NASA Langley, mid 1990s. (NASA Langley and Eglin AF Base)

Mach number = 6, fully turbulent, non-reacting air

CFD performed at 2 Angles of Attack (AoA)

- 0º
- 10º

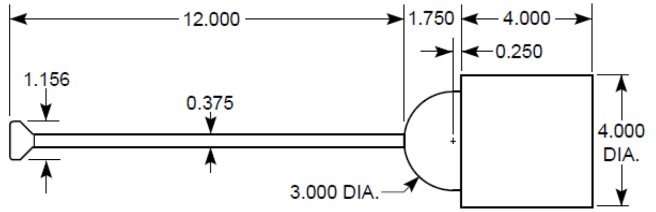

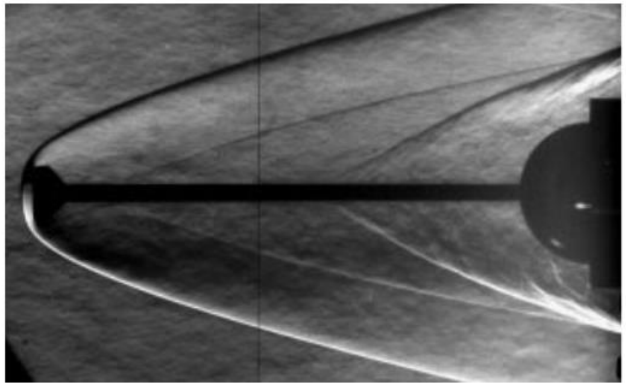

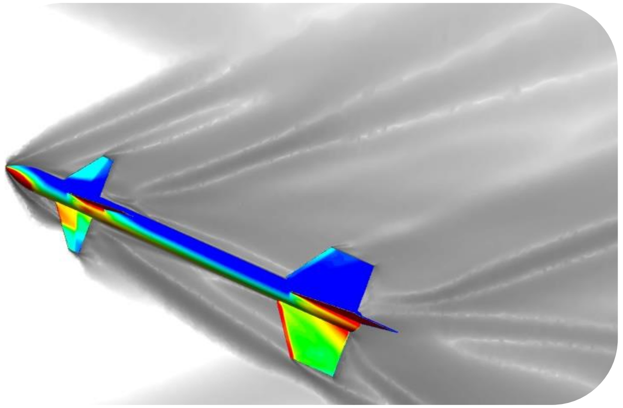

Mach = 6
P_s = 1951 Pa
T_s = 58.25 K
Medium: Air

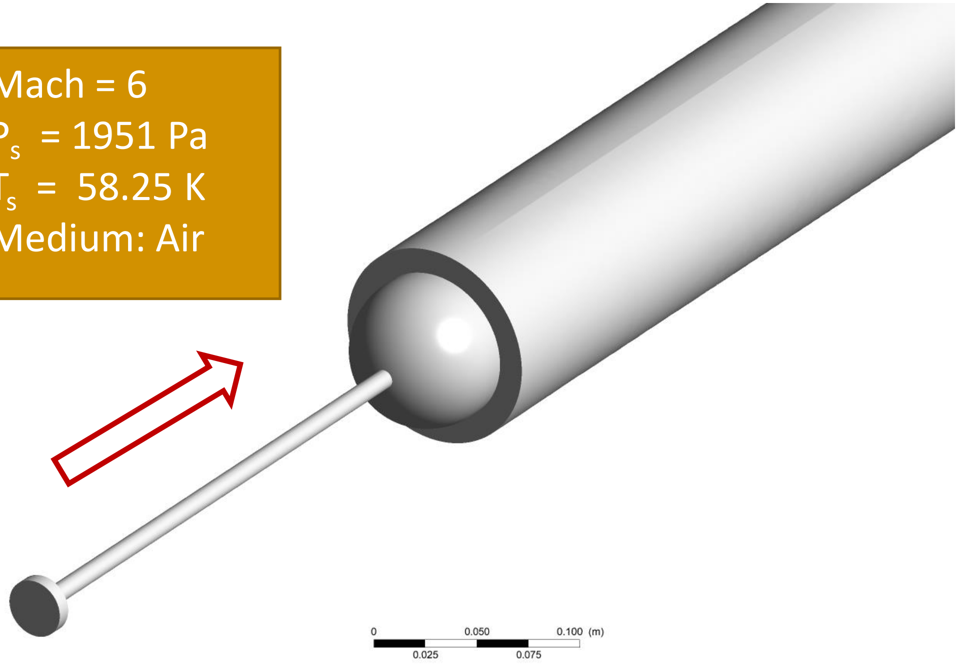

Reference: Huebner, L., et al., Experimental results on the feasibility of an aerospike for hypersonic missiles, 33rd Aerospace Sciences Meeting and Exhibit, Aerospace Sciences Meetings, Reno, NV, 1995.

Case study 1: Validation of Aerospiked Missile at Mach 6

AoA = 10º

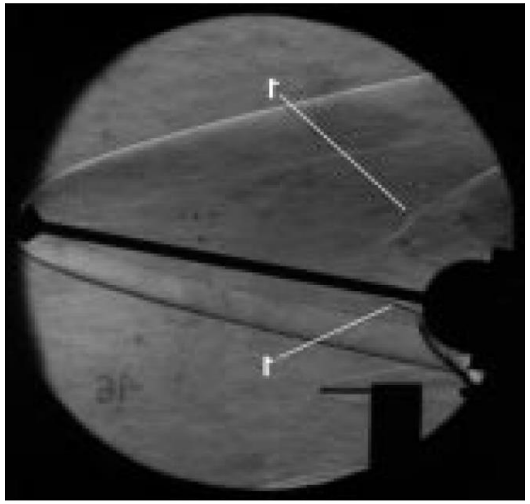

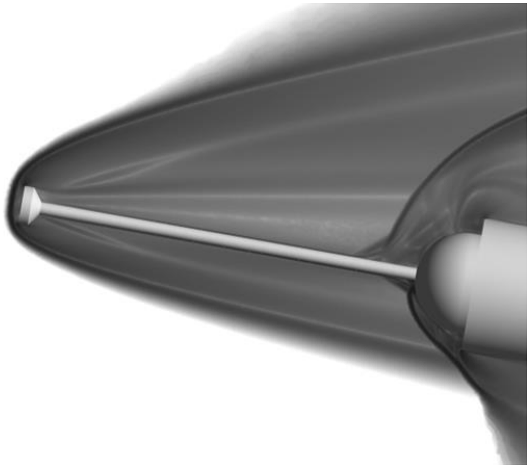

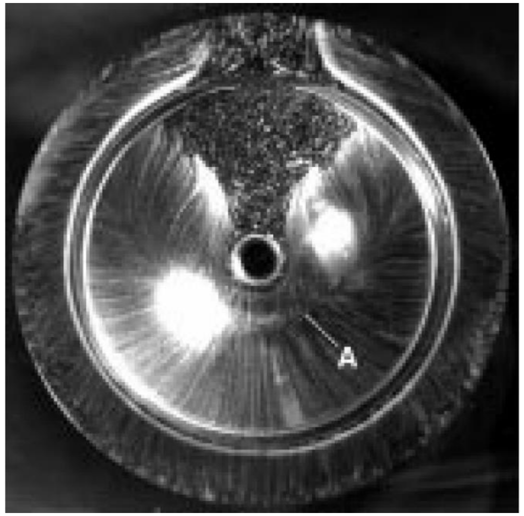

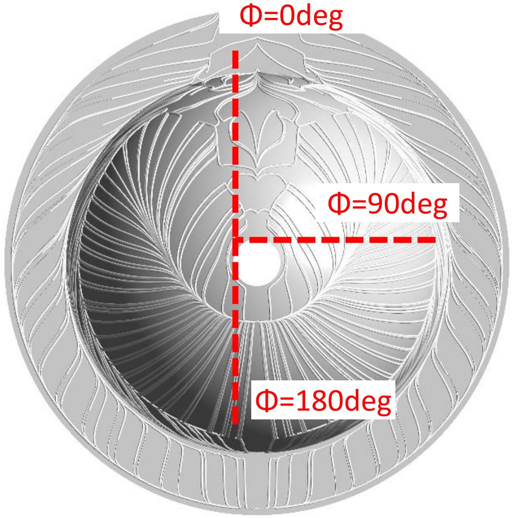

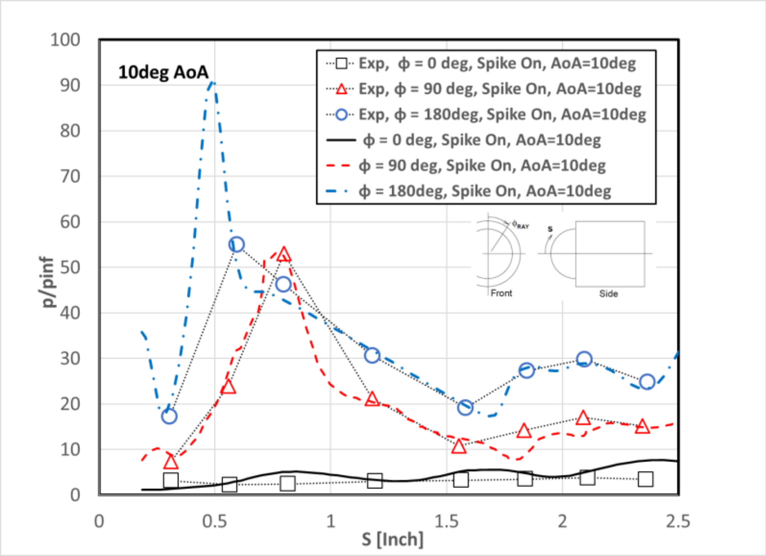

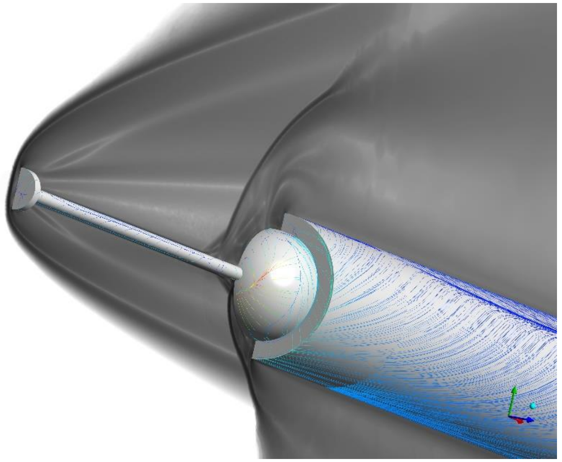

Reference: Rao, V., Viti, V., Abanto, J., "CFD simulations of super/hypersonic missiles: validation, sensitivity analysis and improved design", AIAA 2020-2123, AIAA SciTech 2020, Orlando, FL, January 6-10th, 2020.

Ansys

Case study 1: Validation of Aerospiked Missile at Mach 6

Optimization of Aerodisk using Adjoint solver

Improve performance of aerospike
- Modify only aerodisk shape
- Reduce overall vehicle drag (Target: -2%)
- Keep leading shock away from radome

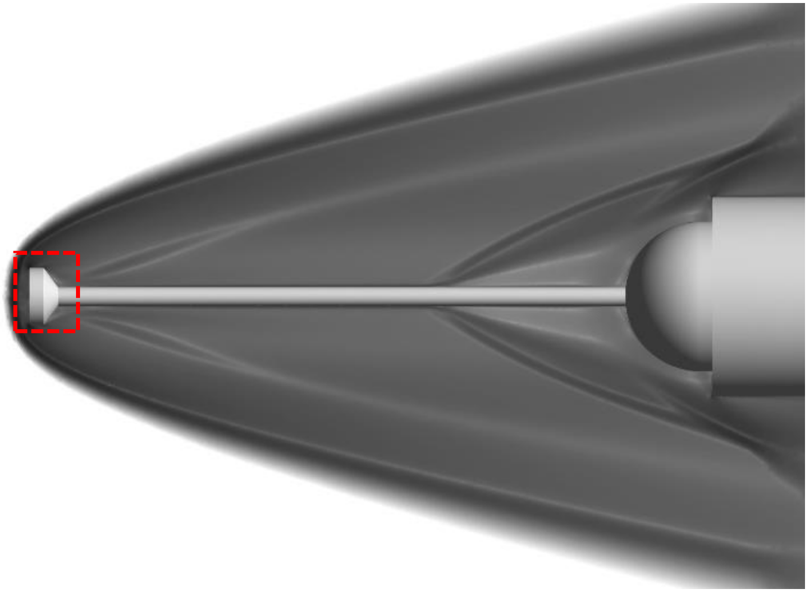

Original

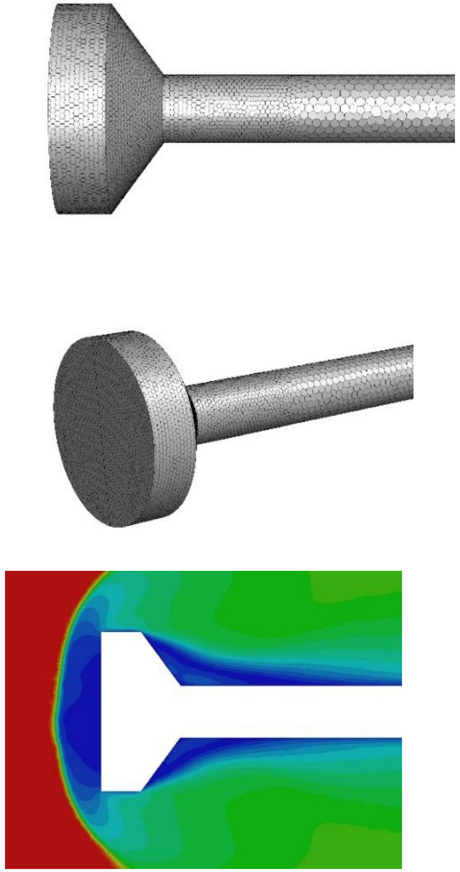

Drag = 95.7 N

Optimized

(2 Adjoint iterations)

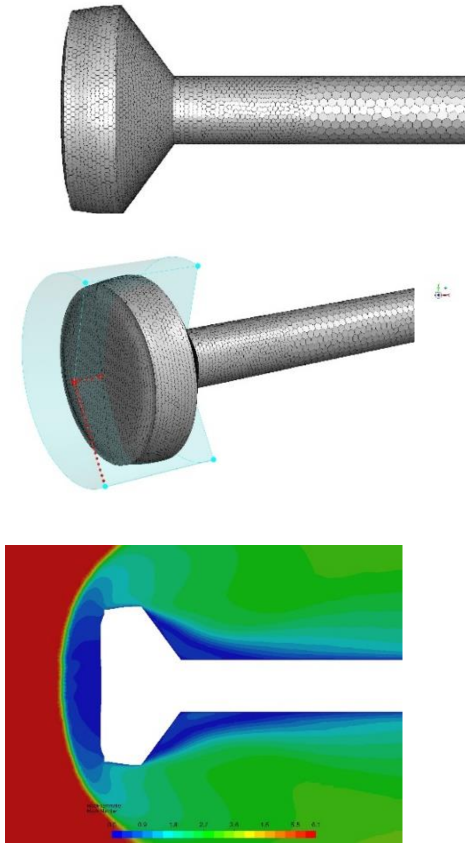

Drag = 94.1 N

Reference: Rao, V., Viti, V., Abanto, J., "CFD simulations of super/hypersonic missiles: validation, sensitivity analysis and improved design", AIAA 2020-2123, AIAA ScitTech 2020, Orlando, FL, January 6-10th, 2020.

Case study 2: Mach 29 Flow Over a Sphere

- Laminar flow over 60.96 mm diameter hemisphere
- Free-stream static pressure and temperature:
  p_s = 12.21 Pa, T_s = 196.7 K
- Laminar finite-rate model to compute chemical sources in energy equation: Gupta model
- Reacting dissociated mixture of 11 species and 21 reactions
  (N_2, O_2, O, N, NO, N^+, O^+, NO^+, N_2^+, O_2^+, e^-)
- Isothermal 1500 K condition at sphere wall
- Structured 2-D mesh: 64,00 quad cells
- Assume axisymmetric flow

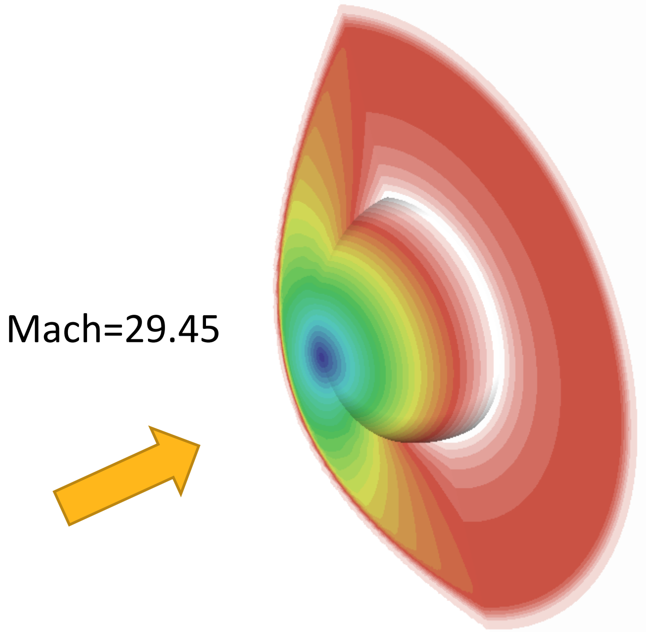

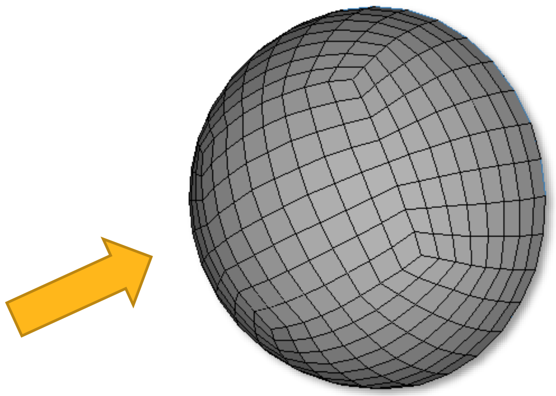

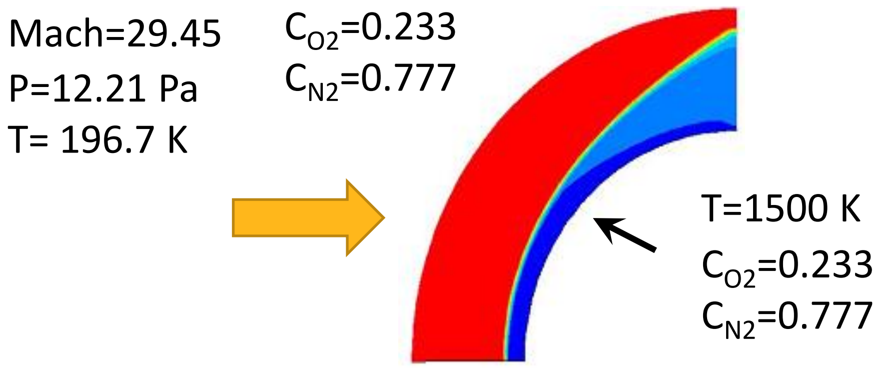

References:
Widhopf, G. F., and Wang, J. C. T., "A TVD Finite-Volume Technique for Nonequilibrium Chemically Reacting Flows", AIAA Paper 1988-2711.
Dellinger, T. C., "Computation of Nonequilibrium Merged Stagnation Shock Layers by Successive Accelerated Replacement", AIAA Journal, 9(2):262-269, 1971.
Kurbatskii, K.A, Kumar, R., and Mann, D., "Simulation of External Hypersonic Problems Using FLUENT 6.3 Density-Based Coupled Solver", 2nd European Conference for Aerospace Sciences

Case study 2: Mach 29 Flow Over a Sphere

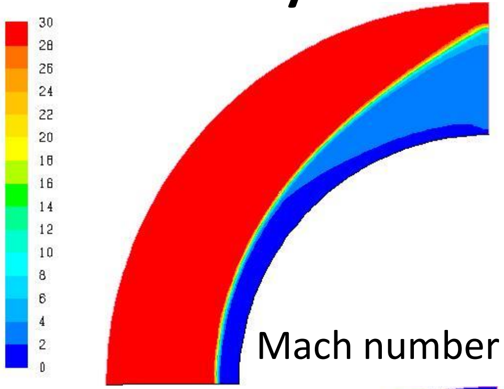

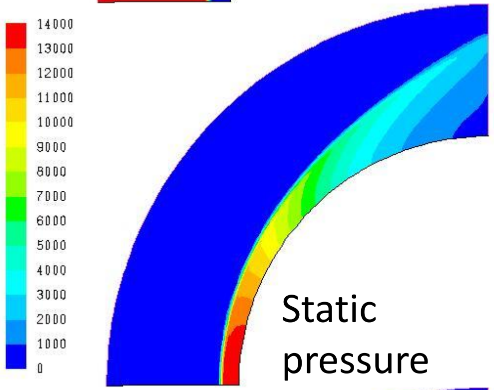

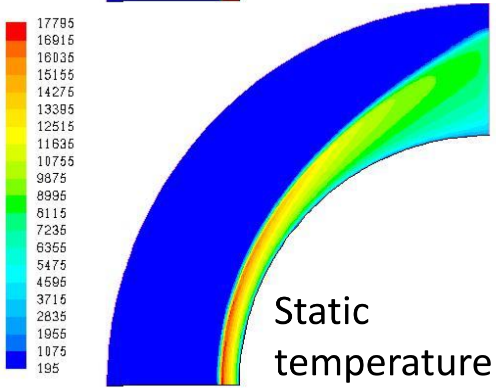

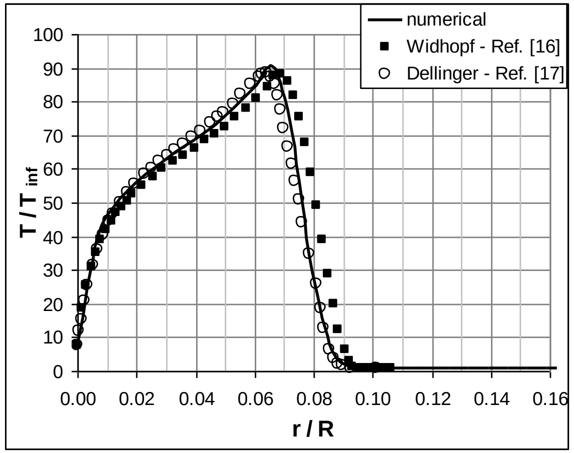

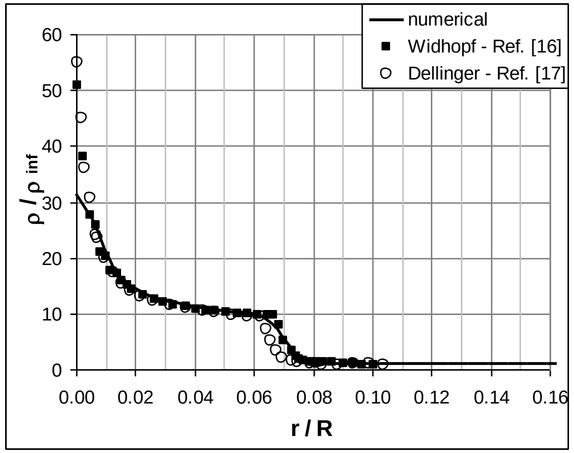

Distributions of normalized static temperature, density, and mass fraction of O_2, O and N_2 along the stagnation streamline

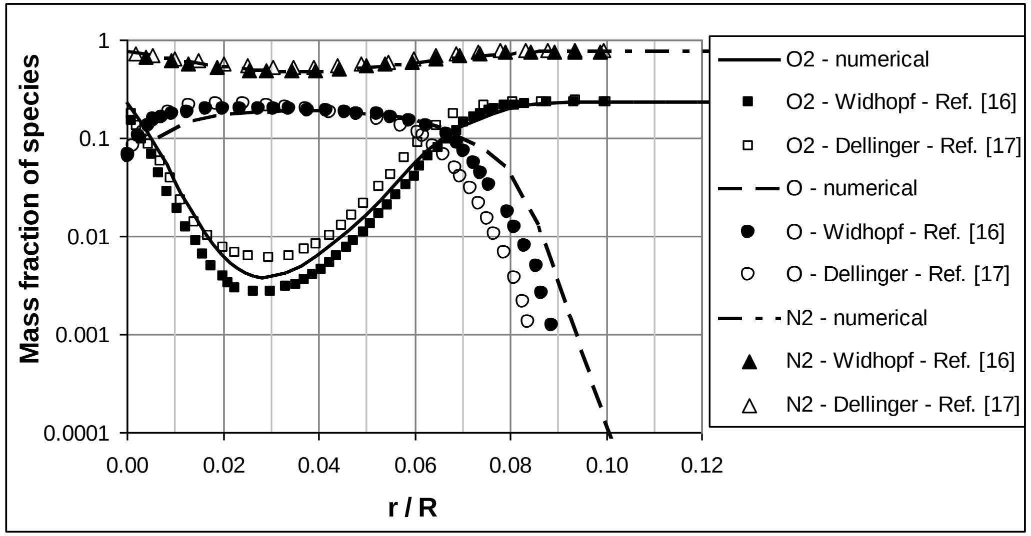

Case study 3: SCRAMJET design fc

Hypersonic technology demonstrator vehicle (HSTDV) testec

Initial validation on scaled-down wind tunnel model

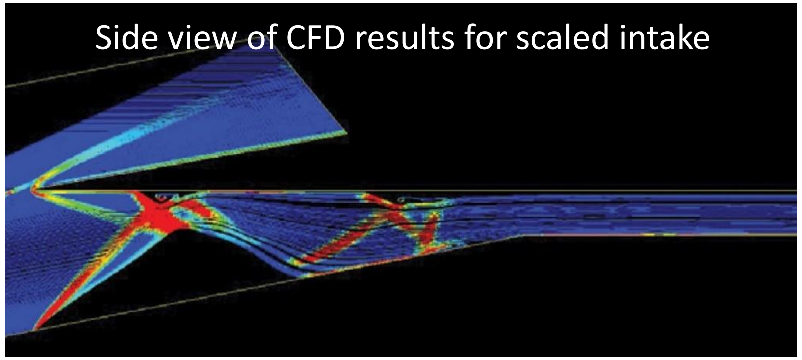

Validation of pressure recovery for 2 cowl angles

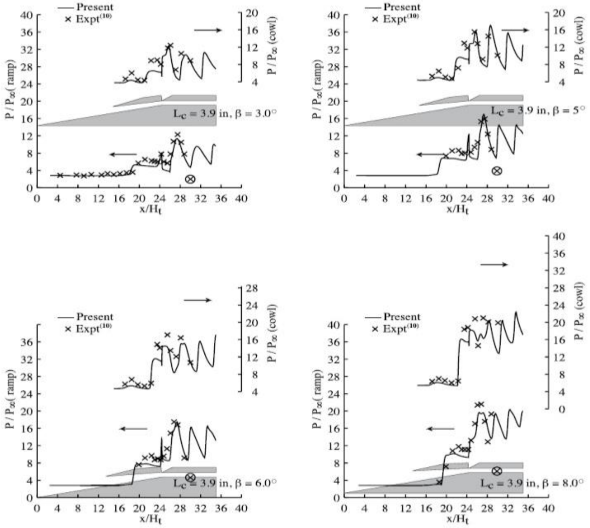

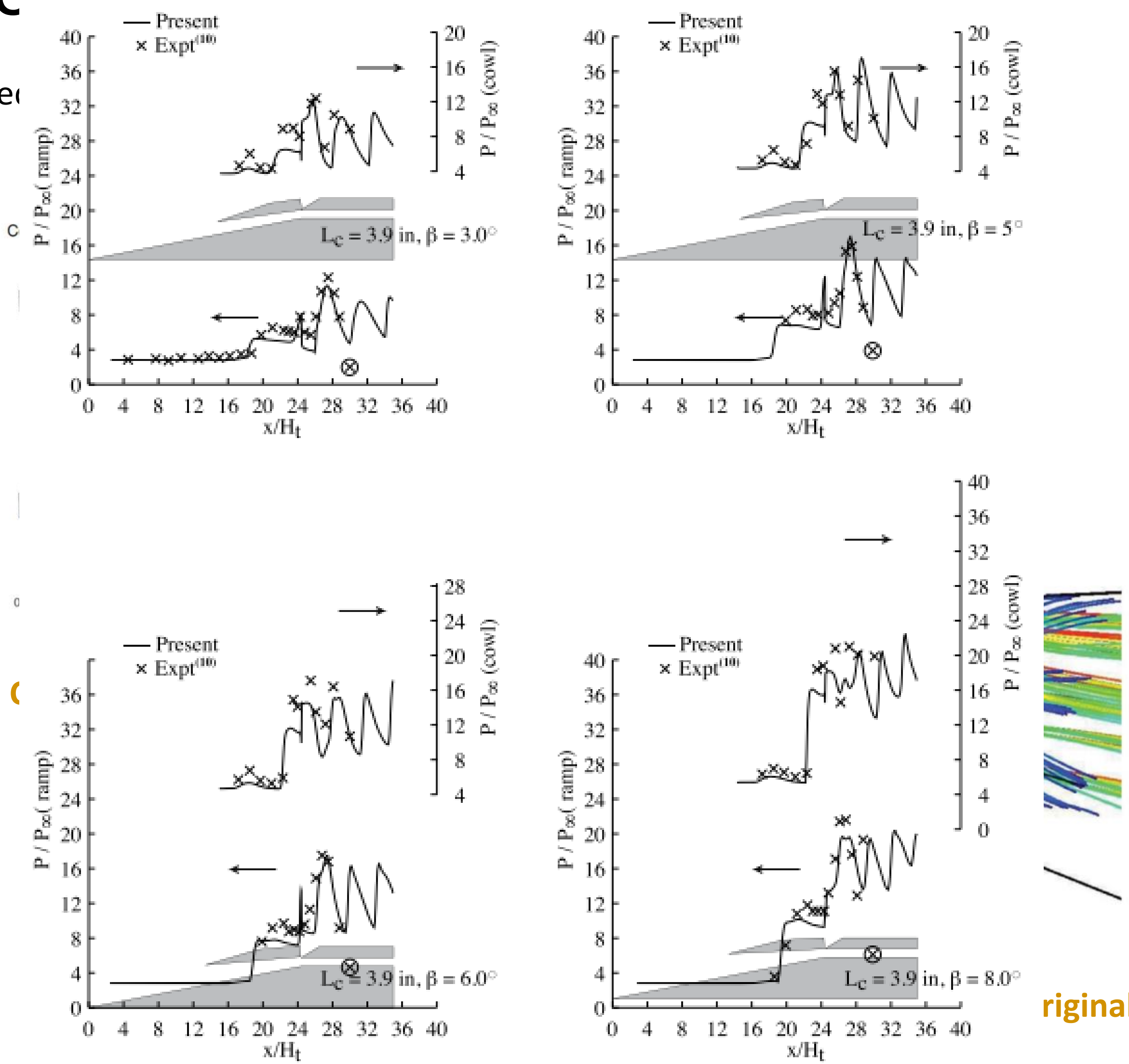

riginal

Reference: V Babu, "Flight like the wind", ANSYS Advantage, Vol.8, 2014

Case study 3: SCRAMJET design for Mach 6.5 cruise

Hypersonic technology demonstrator vehicle (HSTDV) tested and simulated at IIT Madras by Professor V. Babu

Initial validation on scaled-down wind tunnel model

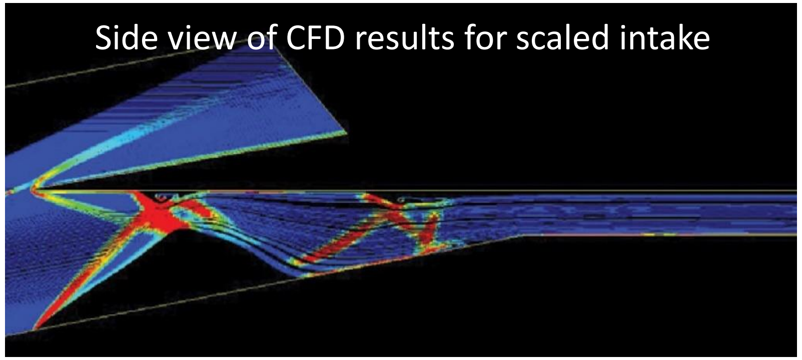

Validation of pressure recovery for 2 cowl angles

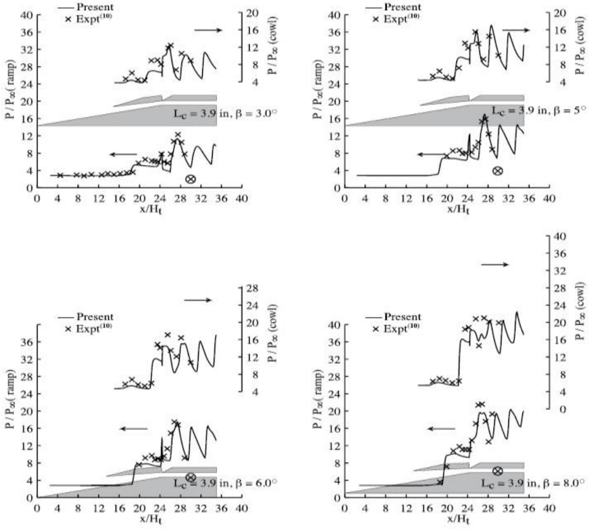

Modified full-scale design of the combustor

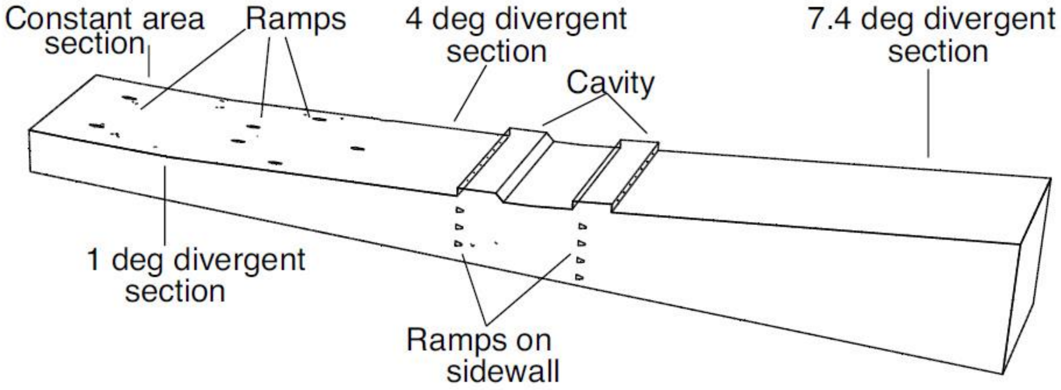

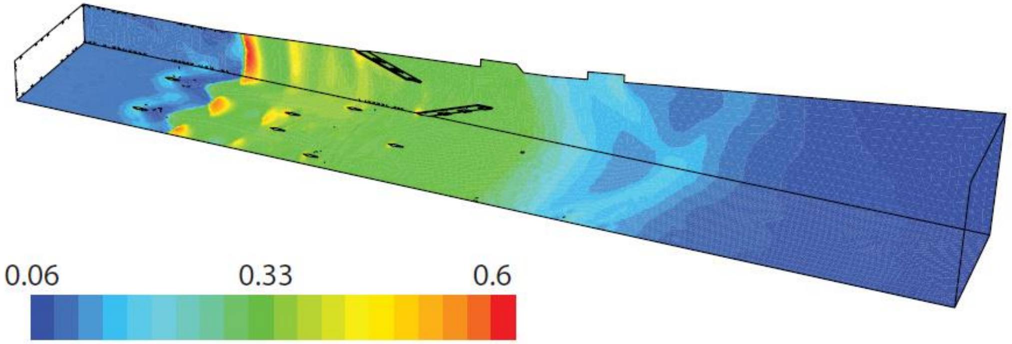

Reference: V Babu, “Flight like the wind”, ANSYS Advantage, Vol.8, 2014

Case study 3: SCRAMJET design for Mach 6.5 cruise

Virtual Wind Tunnel

Hypersonic technology demonstrator vehicle (HSTDV) tested and simulated at IIT Madras by Professor V. Babu

Initial validation on scaled-down wind tunnel model

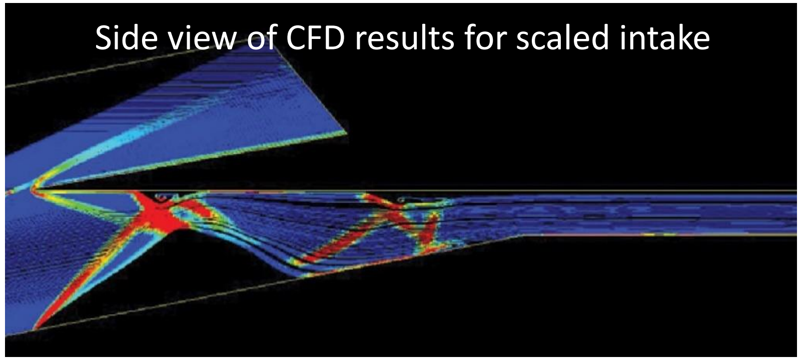

Validation of pressure recovery for 2 cowl angles

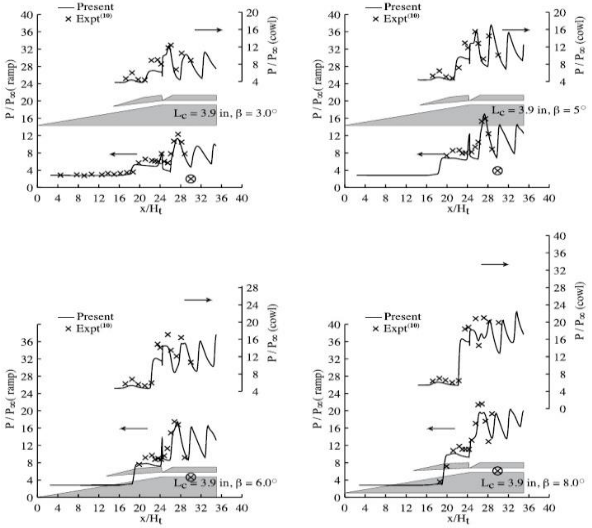

Pressure recovery of final design: experiment and CFD

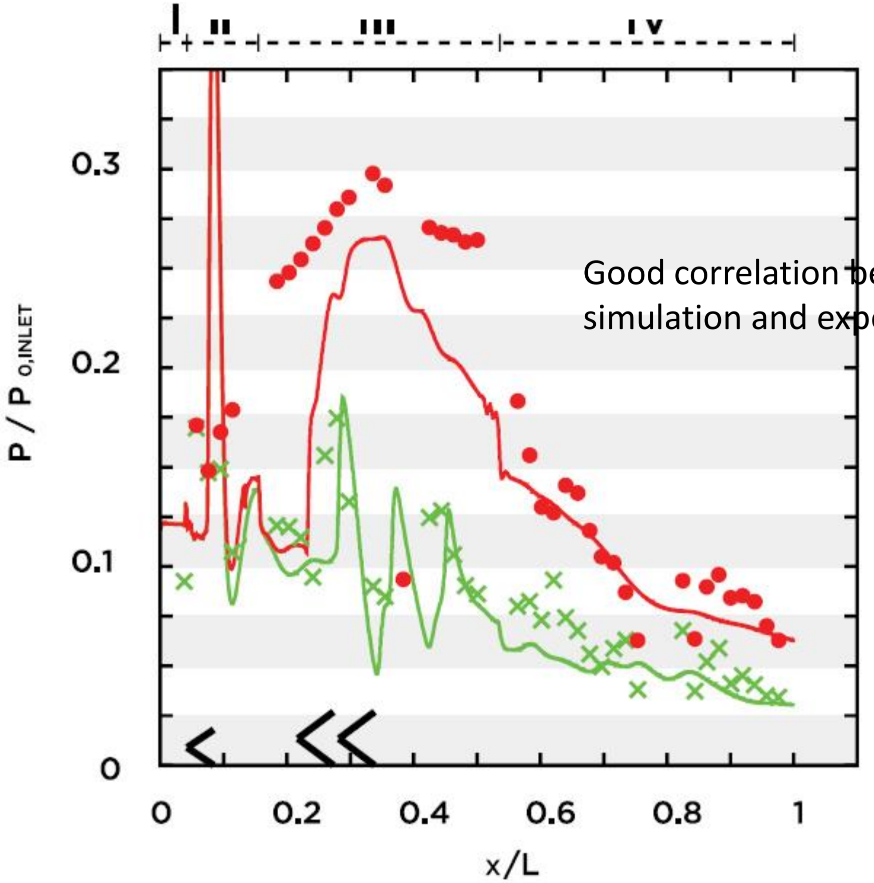

Good correlation between simulation and experiments.

Ansys Hypersonic Fluid-Structure Interaction (FSI) Workflow

Ansys capabilities

- Breadth and depth of physics
- Open platform; can integrate other tools/solvers
- Tool connectivity and Inter-operability
  (FSI, Emag, Systems, Digital Twin)
- Multiphysics ease of use
- Optimization across all tools

Areas of Improvement

- Generic solver, not specific to Hypersonics
- Lacking some hypersonic-specific

capabilities (Development aware, requirements shared)

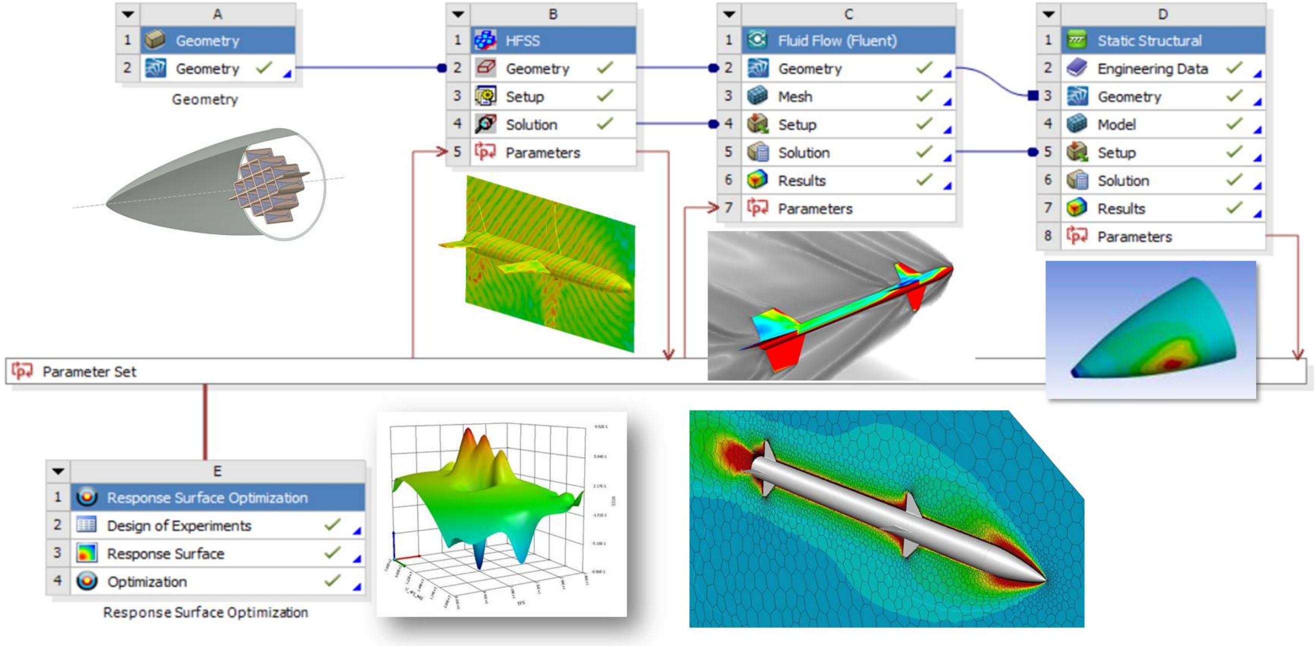

Case Study 4: Projectile Structural Deformation at Mach 10

Hypersonic FSI Workflow

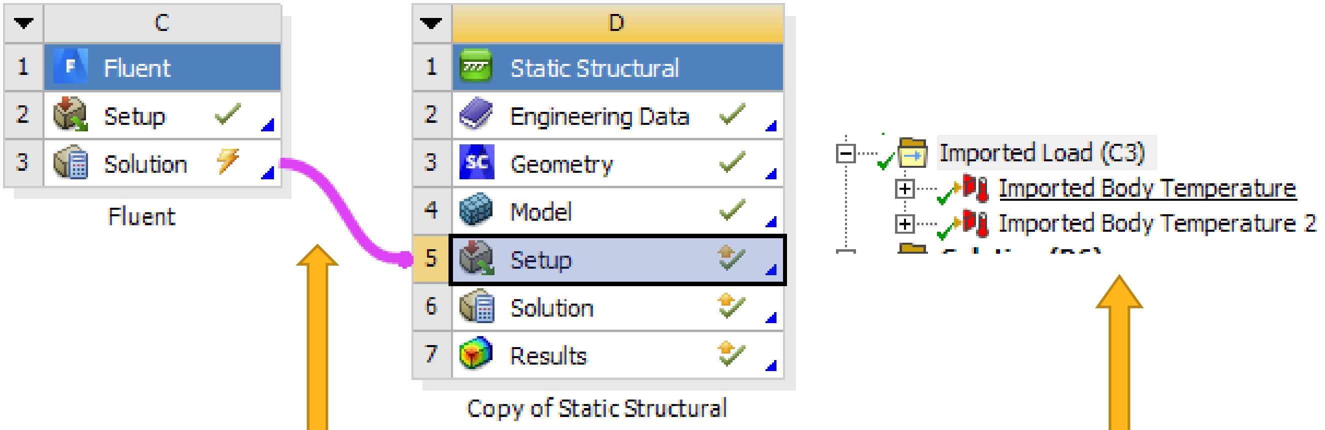

Drag and drop FSI setup

Automated import of files from fluids solver

Fluid-structural deformation under thermal and pressure forces

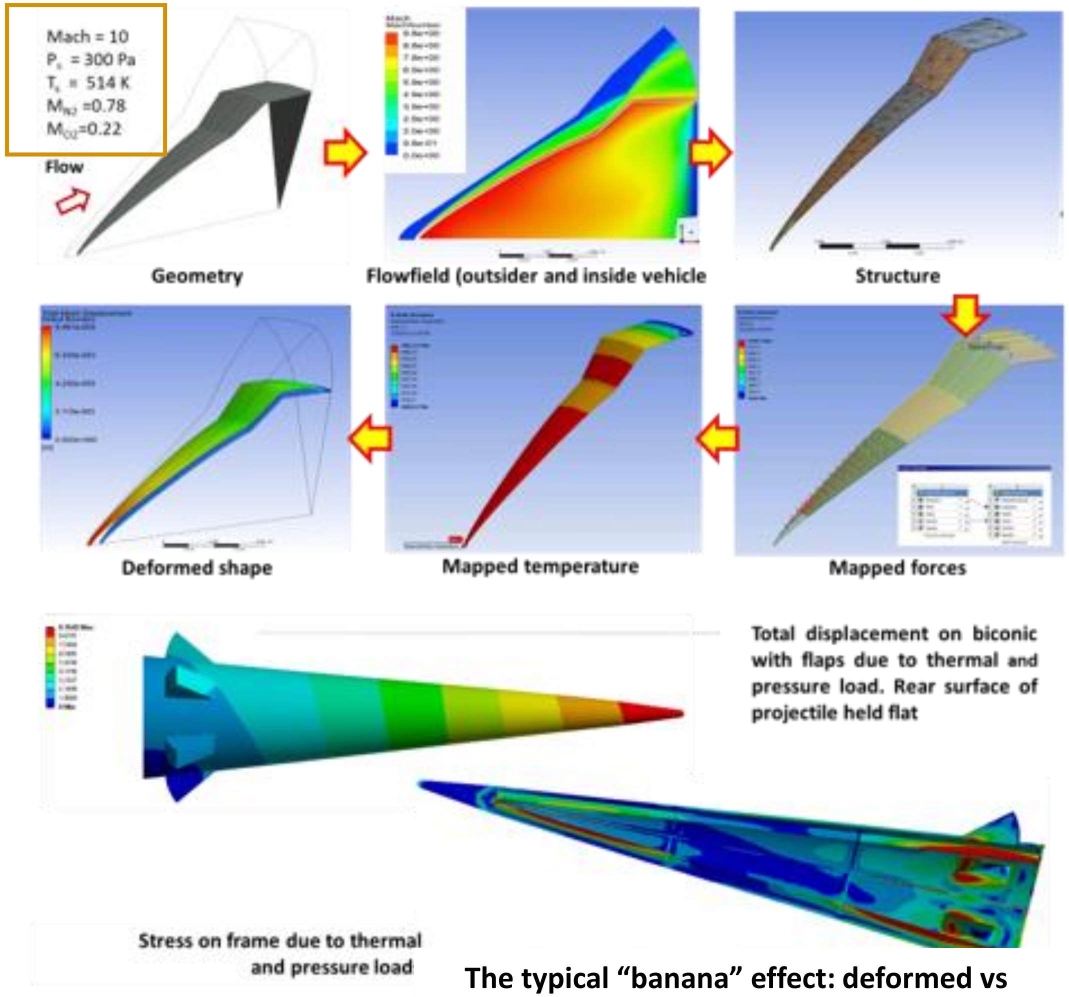

The typical "banana" effect: deformed vs undeformed vehicle shape

Ref: "*Development and validation the ANSYS hypersonic prototype*", Viti et al., Hypersonic Technology and Systems Conference, Alexandria, VA, 26-29 August, 2019.

Case Study 4: Projectile Structural Deformation at Mach 10

Hypersonic FSI Workflow

Fluid data can be mapped from:

- Ansys fluid solver(s)
- 3rd party solvers
- Generic data files

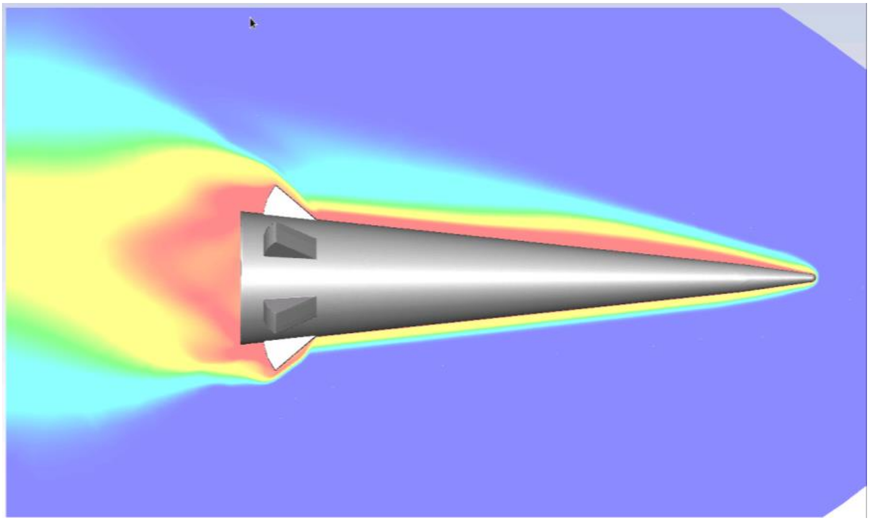

Mapping fluid solution to mechanical solution

Temperature

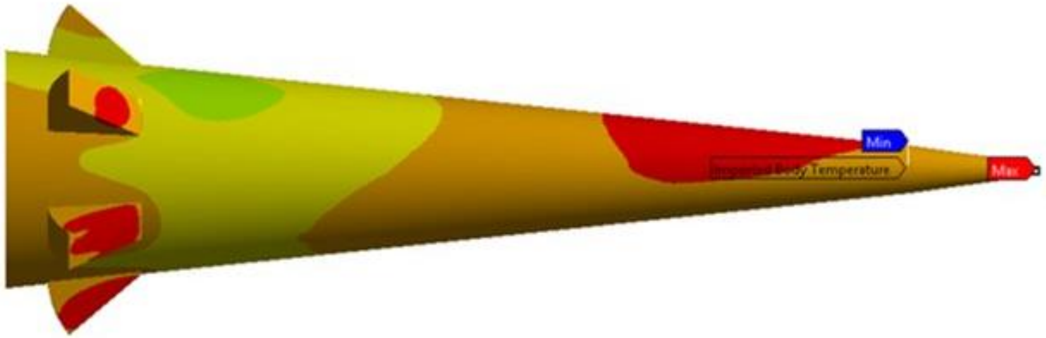

Pressure

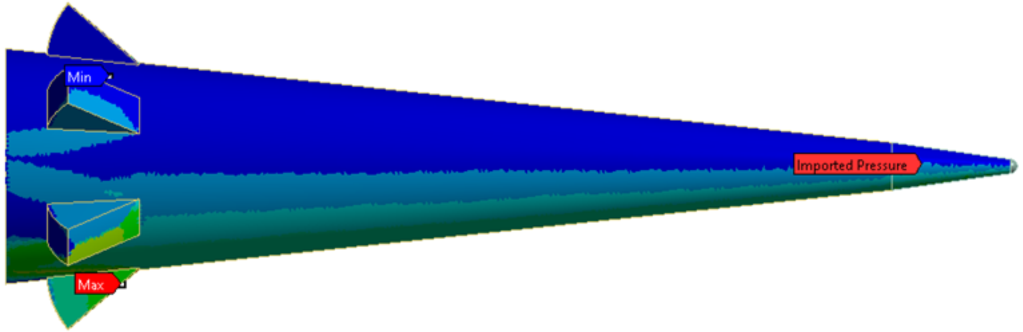

Case Study 4: Projectile Structural Deformation at Mach 10

Structural Displacement for Mach 10: Temps

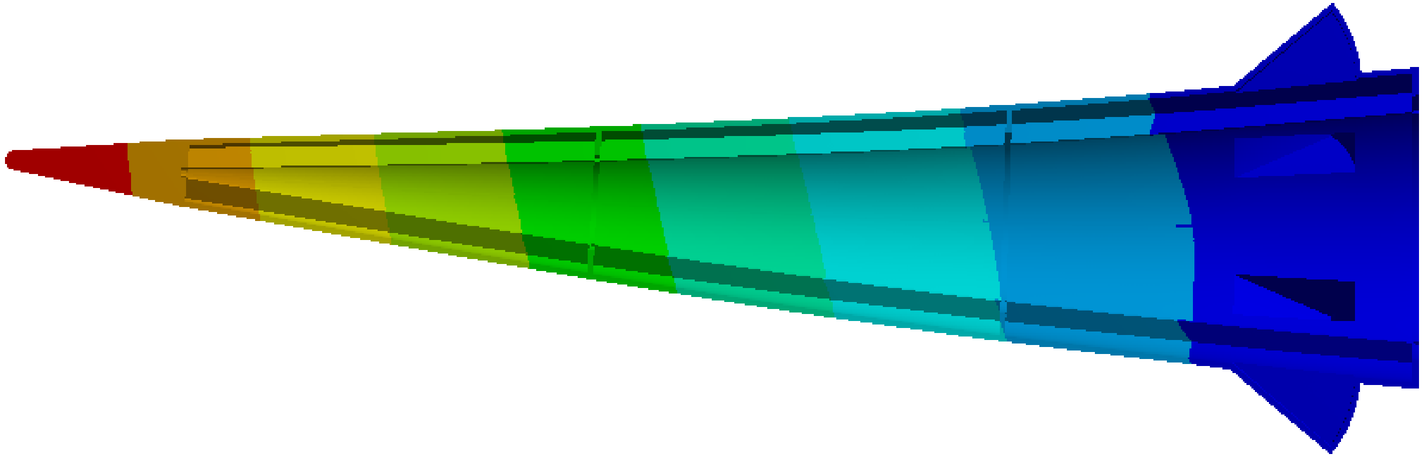

*Displacement field predicts expected curved shape (3x scaling)

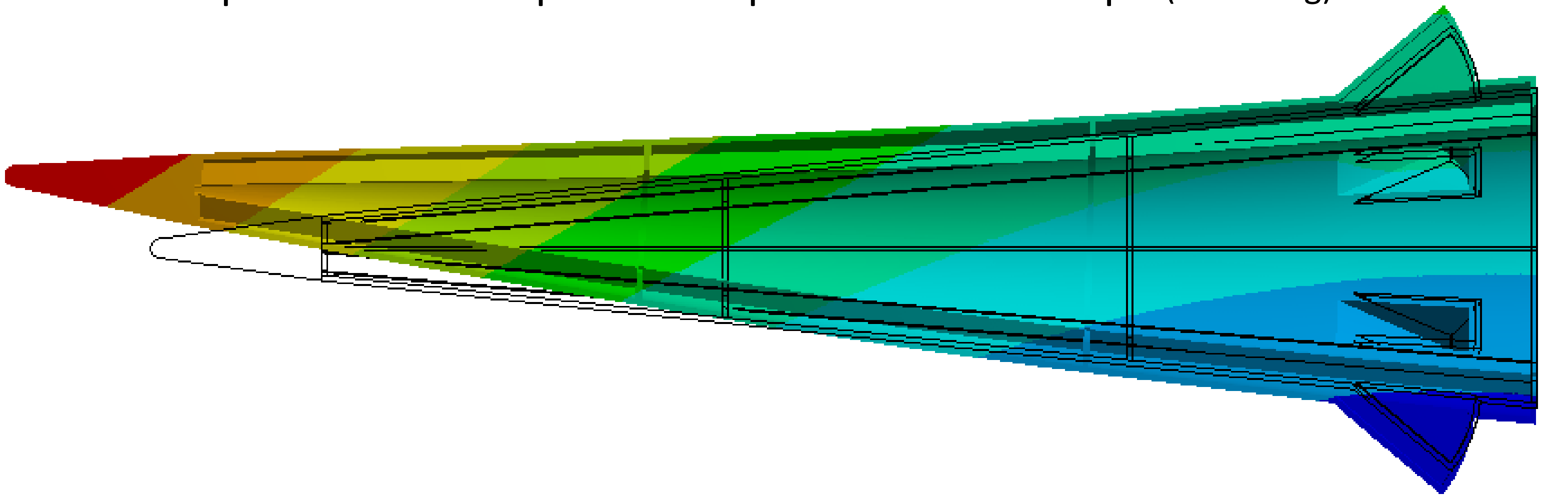

Ansys Technology Stack for Hypersonics

Aerodynamics	Propulsion	Materials & Structures	Communication & Tracking	System Integration

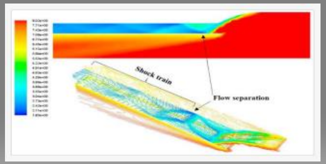

Dual combustion RAMJET

- Transient behavior
- Reduced/order modeling for compressor/turbine

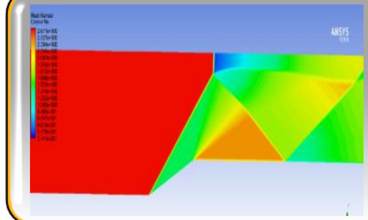

Airframe/propulsion integration and inlet design

- Pressure recovery
- Shock train analysis: impingement and reflection
- Wave riding
- Structural deformation: FSI

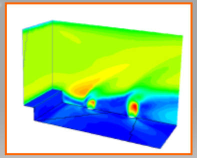

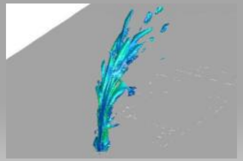

Fuel Injection

- Gaseous, liquid and solid fuel
- Liquid jet breakup
- Mass tranfers

Source: NASA

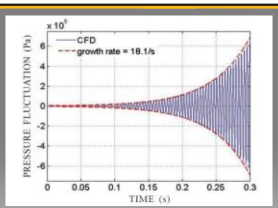

Acoustics and instabilities

- Transient pressure waves
- Resonant frequencies

Nozzle design/plume

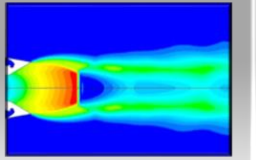

- Over/under-expanded jets
- Plume composition
- Nozzle erosion and solid accumulation

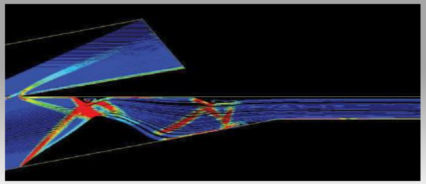

RAM/SCRAMJET Combustion

- Species transport, finite-rate reactions
- Equilibrium and non-equilibrium
- Turbulence Combustion Interaction (TCI)

Thermal cooling technologies

- Radiation, Convection, Conduction
- Multiphase and phase change: boiling, evaporation/condensation
- Jet impingement

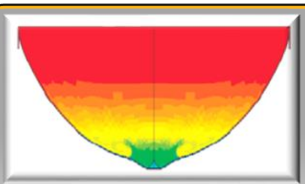

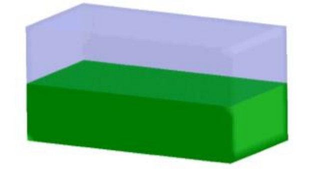

Cryogenic fuel storage and sloshing

- Phase change: evaporation, condensation and boiling
- Heat transfer
- Forces on walls and baffles

Ansys Technology Stack for Hypersonics

Aerodynamics | Propulsion | **Materials & Structures** | Communication & Tracking | System Integration

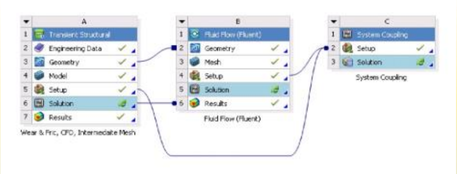
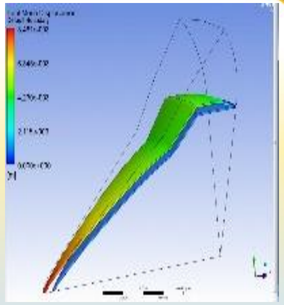

FSI: thermal and pressure loads

- Integrate thermal & mechanical loads
- Extreme thermal gradients (cryogenic fuels to high temperature surfaces) – flutter behavior
- Automated data exchange between physics

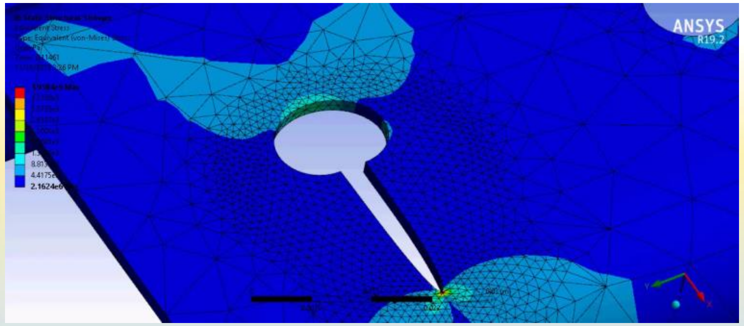

Fracture & Fatigue

- Crack formation & propagation
- Thermal cycling

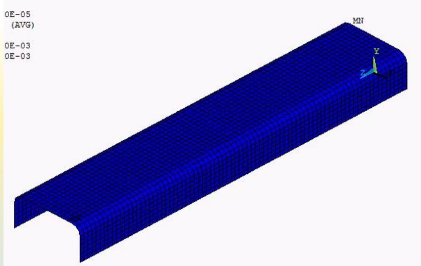

Non-linear Material Behavior

- Creep (stress relaxation)
- Buckling
- Ablation

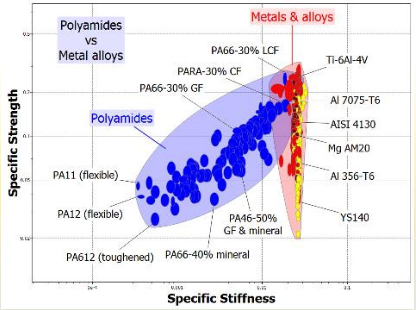

Material Intelligence

- Manage complex material properties – temperature dependence of stiffness, strength
- ICME (Integrated Computational Material Engineering): traceability

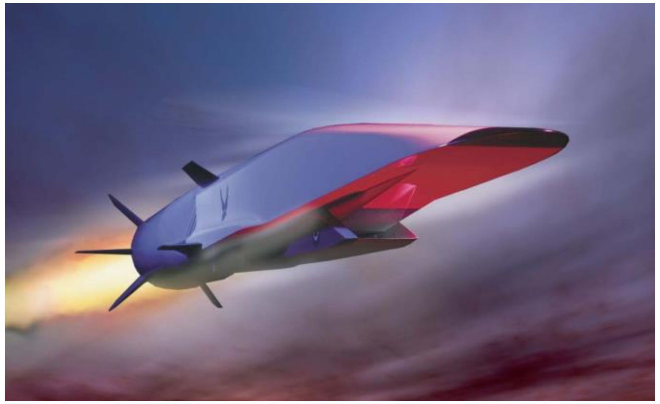

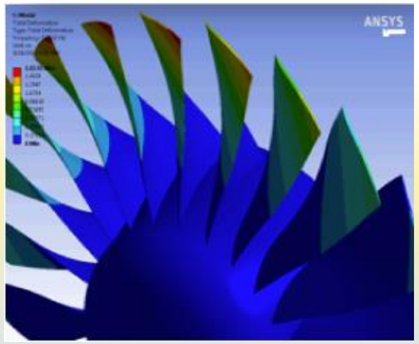

Structural Integrity in Extreme Environment

- Temperature range from -268°C to 2,200°C
- High heat flux (>1,500 W/cm^2)
- Thermal shock (>1,000°C/sec)

Ansys Technology Stack for Hypersonics

Aerodynamics	Propulsion	Materials & Structures	Communication & Tracking	System Integration

Radio and GPS Jamming
- Intentional & Co-site
- Beam Steering

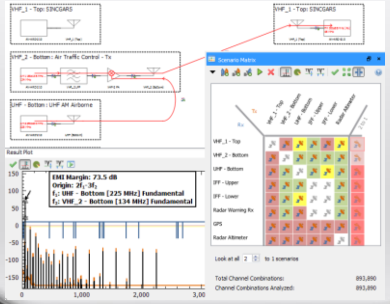

Thermal/Structural impact
- Radome & Electronics

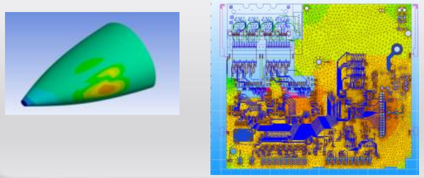

Electronics
- SI/PI, integrated CB
- EI/EC

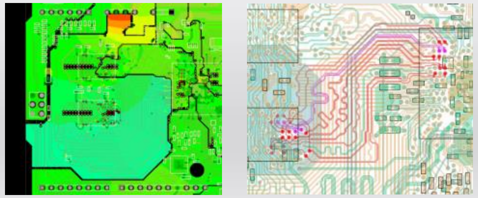

Plasma sheath characterization
- Communication blackout
- Conductive barrier

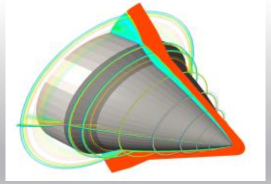

Antennas & Sensors
- Performance degradation
- Effects of aero-heating

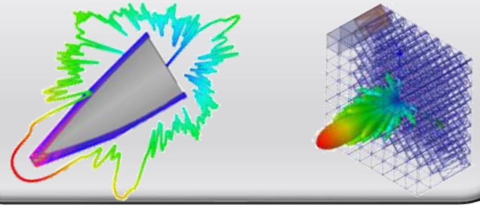

IR Cameras

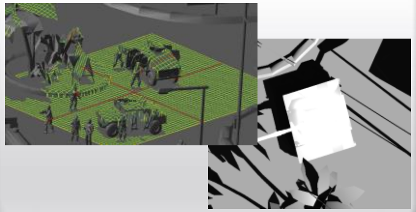

LiDAR signal

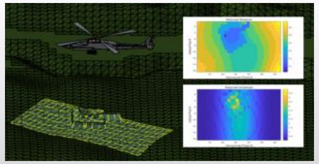

- Field-of-view projected grid
- Time of flight signal

Vibration impact
- Chips, Connectors, Cables

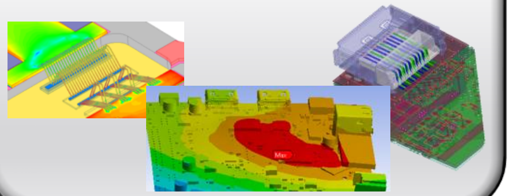

Ansys

Communication Degradation and Blackout: what is it?

- At very high velocities, the temperature increases significantly such that thermally included ionization becomes prevalent
- In the event a plasma exists, it will behave as a metal and cause degradation of RF performance for sensor systems affected
  - Plasma strength depends upon ion density, temperature, neutral species density and will vary strongly spatially
- To accommodate a solution, one would need to include a spatially varying complex conductivity model in Ansys HFSS
- The conductivity will vary significantly in space and needs to be included to capture parasitic effects on RF system

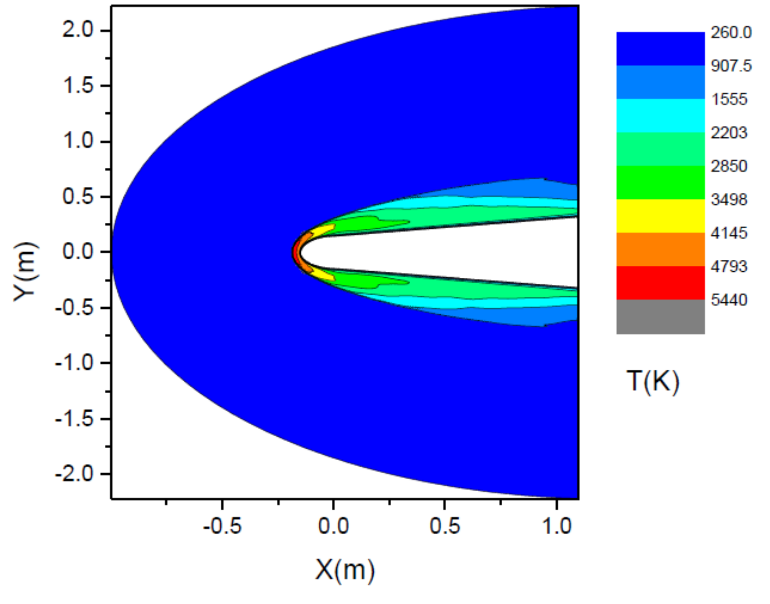

Fig. 3. The temperature distribution of air around the vehicle.

J. Li, M. He, X. Li and C. Zhang, "Multiphysics Modeling of Electromagnetic Wave-Hypersonic Vehicle Interactions Under High-Power Microwave Illumination: 2-D Case," in IEEE Transactions on Antennas and Propagation, vol. 66, no. 7, pp. 3653-3664, July 2018, doi: 10.1109/TAP.2018.2835300.

Extracting Electrical Material Properties of Plasma from Fluent

- Ansys HFSS includes the ability to import 3D Spatially Varying datasets for the definition of material properties
- To create a complex conductivity model, the following is utilized from Ansys Fluent for each spatial location
  - Number Density of Electrons (1/m^3)
  - Number Density of Non-electrons (positive ions and neutral species) (1/m^3)
  - Temperature (K)
- With these values one can use the below, based upon the Drude Model for Free Plasma,

$$\omega_p = \sqrt{\frac{e^2 n_e}{\varepsilon_0 m_e}}$$

$$\nu_c = 6.3\times10^{-15} n_m \sqrt{\frac{T}{300}}$$

$$\sigma(\omega) = \frac{\sigma_o}{1 + j\omega\tau} = \left(\underbrace{\frac{\sigma_o}{1+\omega^2\tau^2}}_{\sigma'(\omega)}\right) - j\left(\underbrace{\frac{\sigma_o\omega\tau}{1+\omega^2\tau^2}}_{\sigma''(\omega)}\right)$$

$$\text{DC Conductivity} = \sigma_0 = \omega_p{}^2\epsilon_0\frac{1}{v}$$

$$\varepsilon_r(\omega,x,y,z) = 1 - \frac{\sigma''}{\omega\epsilon_0}$$

$$\sigma'(\omega,x,y,z) = \frac{\sigma_0}{1+\omega^2\tau^2}$$

- ω_p is the plasma frequency, n_e is the number density of electrons, n_m is the number density of non-electrons
- ν_c is the damping frequency associated with loss = $1/\tau$

Case Study 5: Bringing Ionization Physics into Electrical Analysis

Electromagnetic/Communication/Tracking

- Performance degradation with shape change (side antenna)
- Communication blackout (weakly-ionized gas)

Ansys Hypersonic Prototype: Biconic with flaps

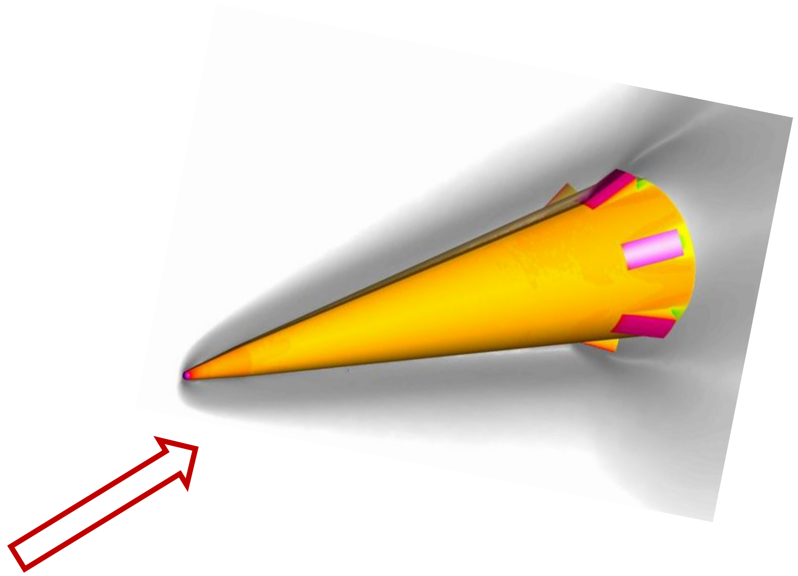

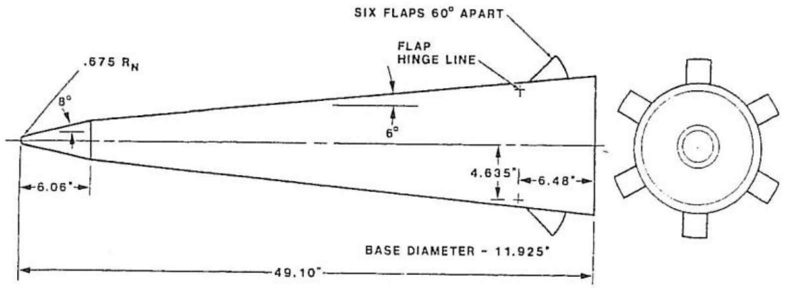

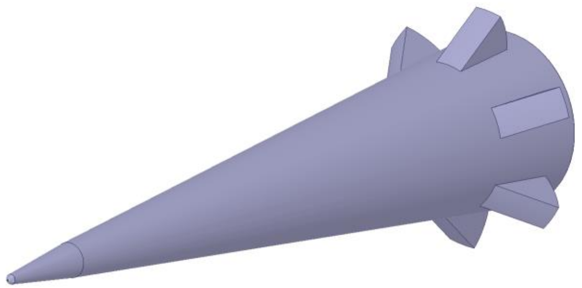

Mach number =20.3, turbulent, reacting air

Altitude ~200k ft

Ps = 36 Pa

Ts = 243 K

AoA = 10 deg

Flap angle = 21 deg

Prototype based on original experimental work at Sandia by Jordan

"Jordan, T.M., Buffington, R.J., Aerodynamic Model for a Hemispherically-Capped Biconic Reentry Vehicle with Six Drag Flaps. AIAA Paper 87-2364, 1987."

Flow Solution

Mach Number Contours for 45° Flap Angle (Mach 10)

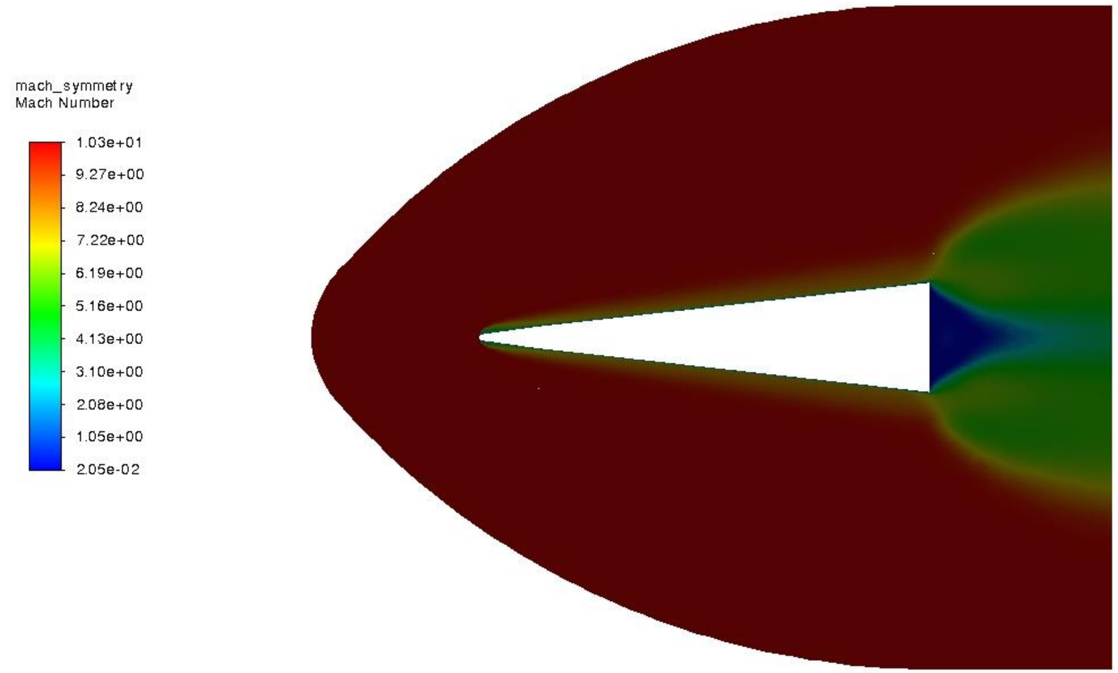

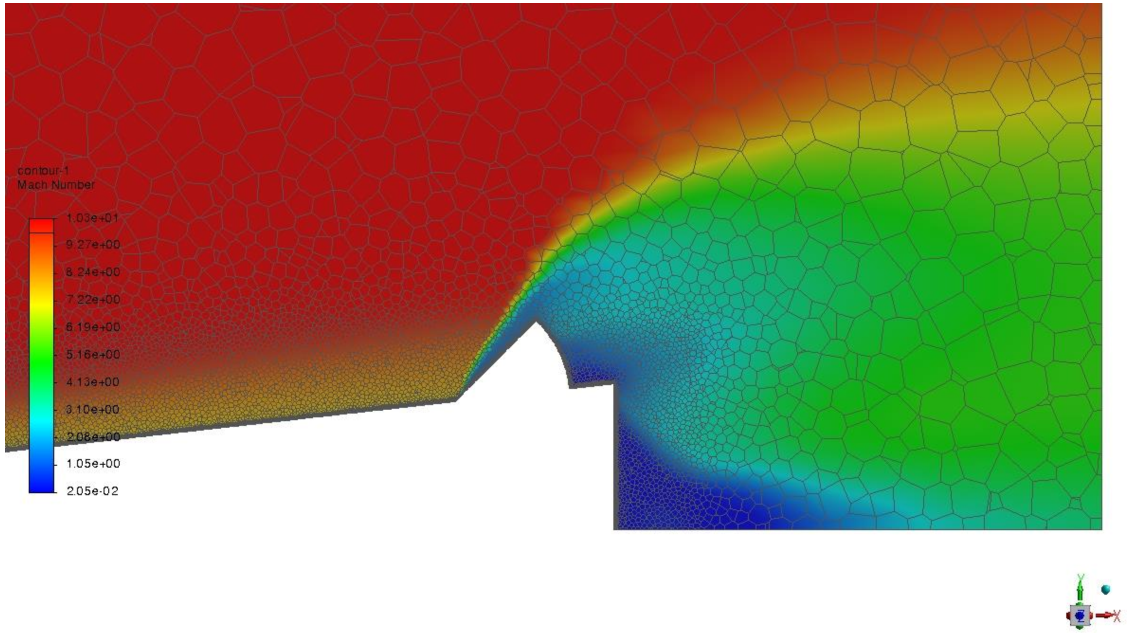

Flow Solution

Air Temperature (Mach 20)

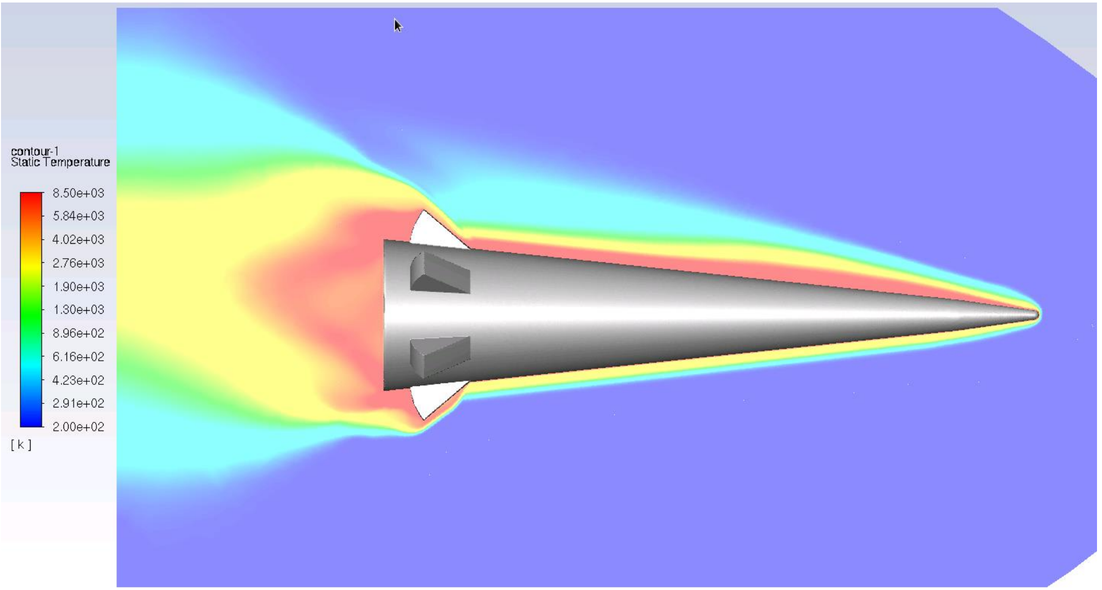

Spatial Variation of Thermally Induced Electron Concentration

Molar Concentration of Electrons (Mach 20)

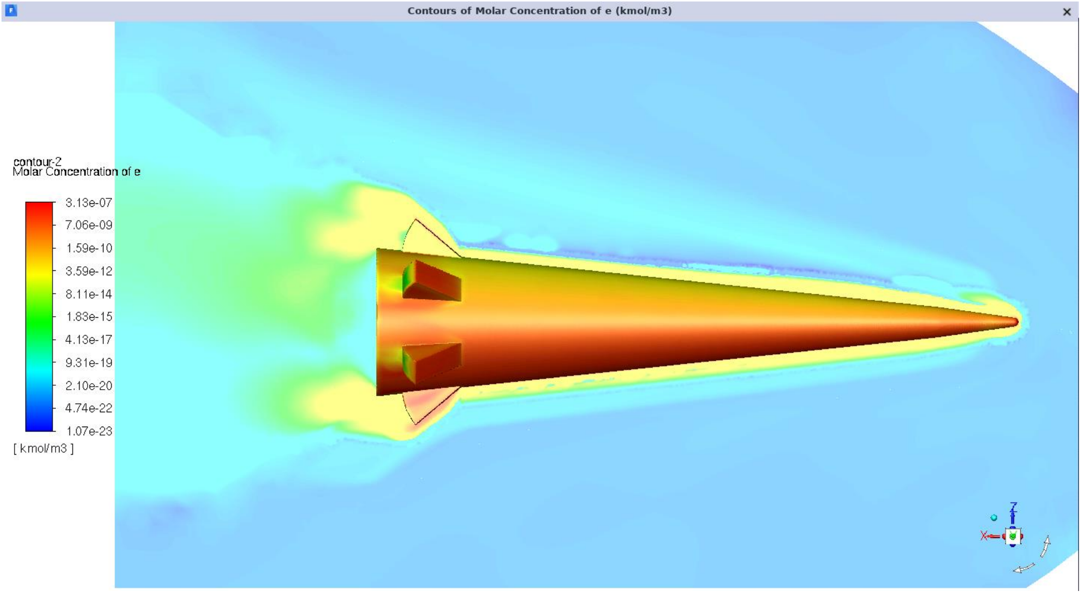

Electromagnetics Solution

Spatially Varying Permittivity and Conductivity (Mach 20)

- Once the datasets are created for permittivity and conductivity, they can be imported.
- Regions of high electron concentration display large negative permittivity
  - Negative permittivity induces evanescent field propagation with a decay length related to the magnitude. If the negative permittivity becomes large, it can decay all signal preventing communication to a receiving antenna.

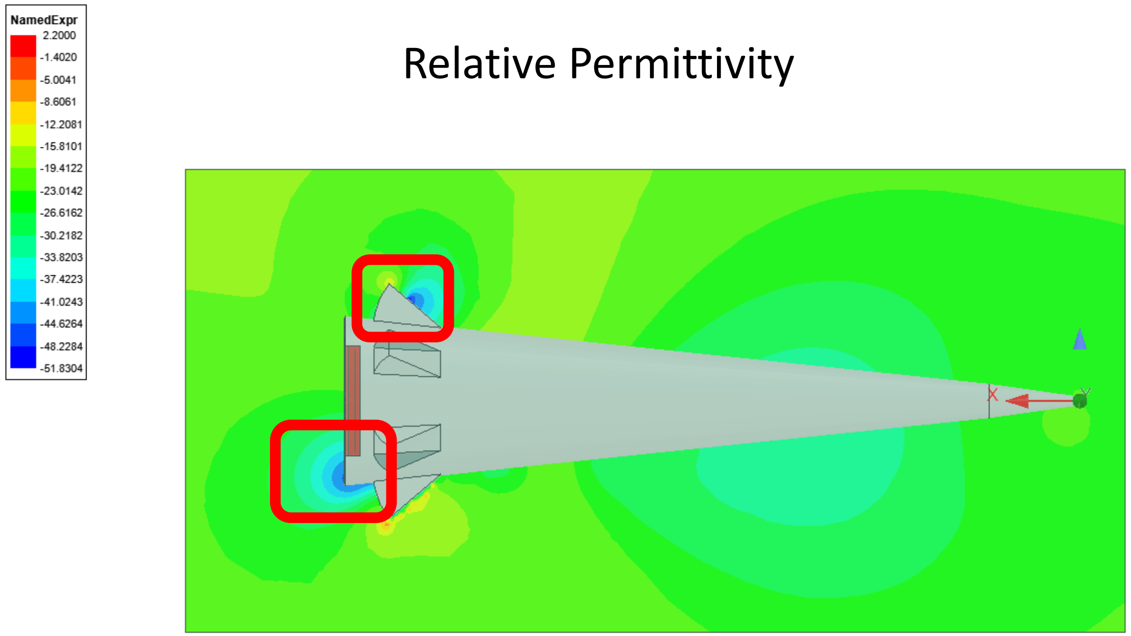

Relative Permittivity

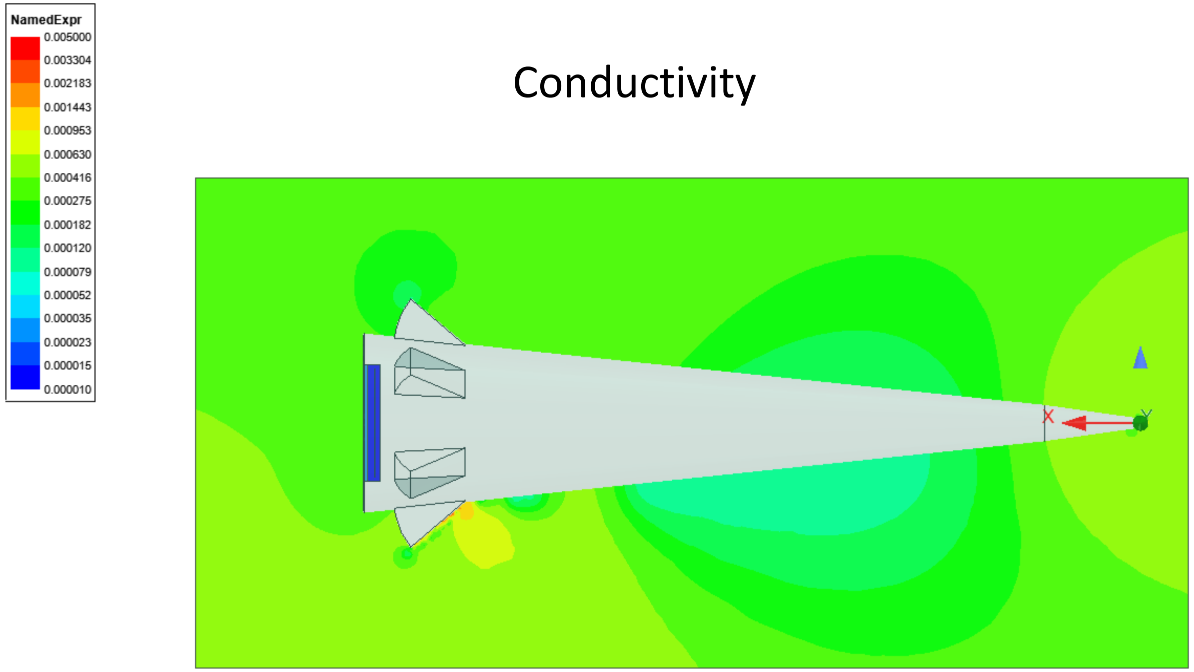

Conductivity

Plasma effects on Antenna Field Generation

Simulated Results and Comparisons (Mach 20)

- A simple bowtie antenna with a dielectric radome was installed in the rear of the projectile
  - Operating Frequency of 300MHz
  - Notice marked degradation of Electric Field propagating into region
    - ➢ Same scales for both field plots

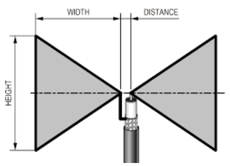

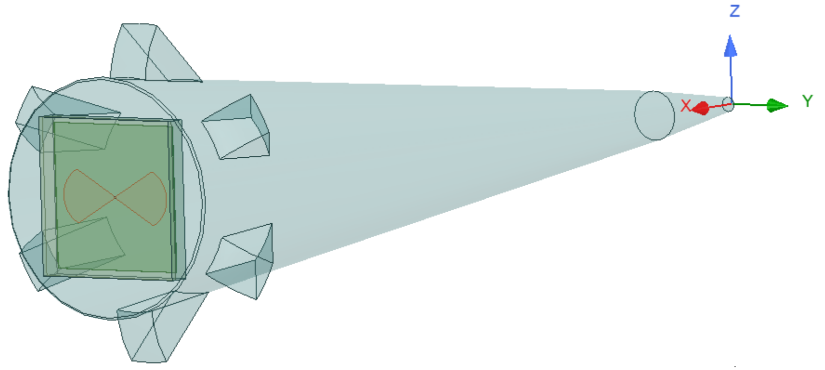

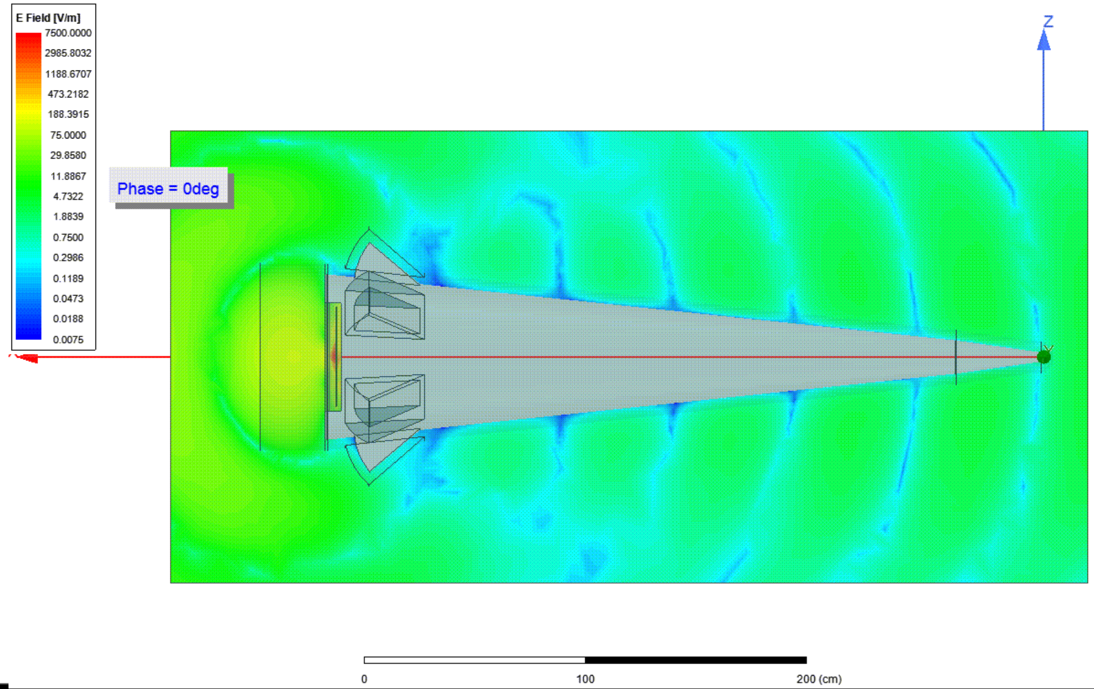

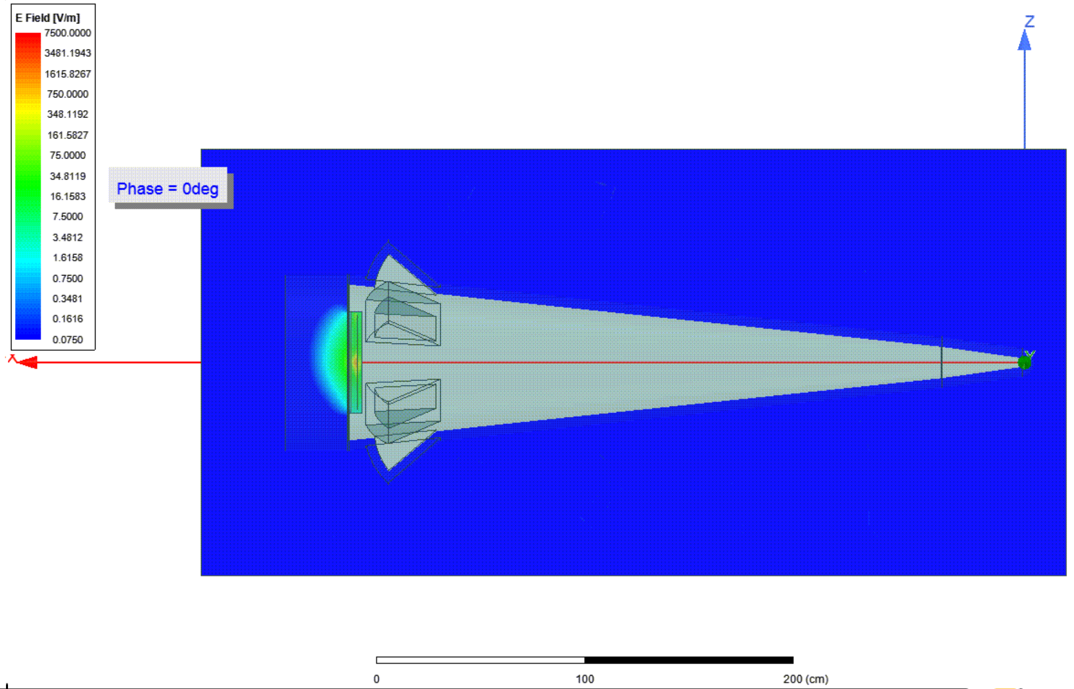

Case Study 6: Hyperboloid re-entry capsule

M = 15.0 (validation done at Mach 10)
P_s = 300 Pa
T_s = 514 K
M_{N2} = 0.78
M_{O2} = 0.22

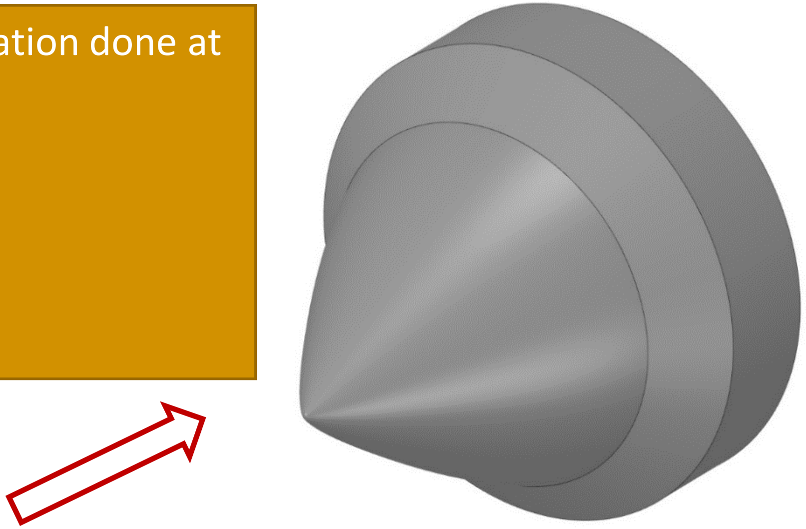

Flare geometry derived from windward center line of Hermes 1.0 Space Plane at 0 deg AoA with 20 deg deflected body flap

- Laminar flow
- Freestream static pressure and temperature: p_s = 300 Pa, T_s = 514 K
- Isothermal 300 K condition at walls
- Block-structured 2D mesh of 34,100 quad cells
- Gas is a reacting dissociated mixture of 11 species in chemical non-equilibrium: N_2, O_2, O, N, NO, NO+, N_2+, O_2+, O+, N+, e-
- Use Gupta chemical reacting model for air, 20 reactions

Table II. Chemical Reactions and Rate Coefficients

Reaction number,* r	Reaction	Forward rate coefficient, $k_{f,r}$, cm³/mole-sec	Backward rate coefficient, $k_{b,r}$, cm³/mole-sec or cm⁶/mole²-sec	Third body M
1	$O_2 + M_1 \rightleftharpoons 2O + M_1$	$3.61 \times 10^{18} T^{-1.0} \exp(-5.94 \times 10^4/T)$	$3.01 \times 10^{15} T^{-0.5}$	O, N, O_2, N_2, NO
2	$N_2 + M_2 \rightleftharpoons 2N + M_2$	$1.92 \times 10^{17} T^{-0.5} \exp(-1.131 \times 10^5/T)$	$1.09 \times 10^{16} T^{-0.5}$	O, O_2, N_2, NO
3	$N_2 + N \rightleftharpoons 2N + N$	$4.15 \times 10^{22} T^{-1.5} \exp(-1.131 \times 10^5/T)$	$2.32 \times 10^{21} T^{-1.5}$	
4	$NO + M_3 \rightleftharpoons N + O + M_3$	$3.97 \times 10^{20} T^{-1.5} \exp(-7.56 \times 10^4/T)$	$1.01 \times 10^{20} T^{-1.5}$	O, N, O_2, N_2, NO
5	$NO + O \rightleftharpoons O_2 + N$	$3.18 \times 10^9 T^{1.0} \exp(-1.97 \times 10^4/T)$	$9.63 \times 10^{11} T^{0.5} \exp(-3.6 \times 10^3/T)$	
6	$N_2 + O \rightleftharpoons NO + N$	$6.75 \times 10^{13} \exp(-3.75 \times 10^4/T)$	1.5×10^{13}	
7	$N + O \rightleftharpoons NO^+ + e^-$	$9.03 \times 10^9 T^{0.5} \exp(-3.24 \times 10^4/T)$	$1.80 \times 10^{19} T^{-1.0}$	
8	$O + e^- \rightleftharpoons O^+ + e^- + e^-$	$(3.6 \pm 1.2) \times 10^{31} T^{-2.91} \exp(-1.58 \times 10^5/T)$	$(2.2 \pm 0.7) \times 10^{40} T^{-4.5}$	
9	$N + e^- \rightleftharpoons N^+ + e^- + e^-$	$(1.1 \pm 0.4) \times 10^{32} T^{-3.14} \exp(-1.69 \times 10^5/T)$	$(2.2 \pm 0.7) \times 10^{40} T^{-4.5}$	
10	$O + O \rightleftharpoons O_2^+ + e^-$	$(1.6 \pm 0.4) \times 10^{17} T^{-0.98} \exp(-8.08 \times 10^4/T)$	$(8.02 \pm 2.0) \times 10^{21} T^{-1.5}$	
11	$O + O_2^+ \rightleftharpoons O_2 + O^+$	$2.92 \times 10^{18} T^{-1.11} \exp(-2.8 \times 10^4/T)$	$7.8 \times 10^{11} T^{0.5}$	
12	$N_2 + N^+ \rightleftharpoons N + N_2^+$	$2.02 \times 10^{11} T^{0.81} \exp(-1.3 \times 10^4/T)$	$7.8 \times 10^{11} T^{0.5}$	
13	$N + N \rightleftharpoons N_2^+ + e^-$	$(1.4 \pm 0.3) \times 10^{13} \exp(-6.78 \times 10^4/T)$	$(1.5 \pm 0.5) \times 10^{22} T^{-1.5}$	
14	$O_2 + N_2 \rightleftharpoons NO + NO^+ + e^-$	$1.38 \times 10^{20} T^{-1.84} \exp(-1.41 \times 10^5/T)$	$1.0 \times 10^{24} T^{-2.5}$	
15	$NO + M_4 \rightleftharpoons NO^+ + e^- + M_4$	$2.2 \times 10^{15} T^{-0.35} \exp(-1.08 \times 10^5/T)$	$2.2 \times 10^{26} T^{-2.5}$	O_2, N_2
16	$O + NO^+ \rightleftharpoons NO + O^+$	$3.63 \times 10^{15} T^{-0.6} \exp(-5.08 \times 10^4/T)$	1.5×10^{13}	
17	$N_2 + O^+ \rightleftharpoons O + N_2^+$	$3.4 \times 10^{19} T^{-2.0} \exp(-2.3 \times 10^4/T)$	$2.48 \times 10^{19} T^{-2.2}$	
18	$N + NO^+ \rightleftharpoons NO + N^+$	$1.0 \times 10^{19} T^{-0.93} \exp(-6.1 \times 10^4/T)$	4.8×10^{14}	
19	$O_2 + NO^+ \rightleftharpoons NO + O_2^+$	$1.8 \times 10^{15} T^{0.17} \exp(-3.3 \times 10^4/T)$	$1.8 \times 10^{13} T^{0.5}$	
20	$O + NO^+ \rightleftharpoons O_2 + N^+$	$1.34 \times 10^{13} T^{0.31} \exp(-7.727 \times 10^4/T)$	1.0×10^{14}	

*Reactions and reaction rates for numbers 1 to 7 are from Blottner's (ref. 17) 7-species chemical model and those for numbers 8 to 20 are from reference 21.

Gupta, R. N., Yoss J.,Thompson, R., Lee, K., A Review of Reaction Rates and Thermodynamic and Transport Properties for an 11-Species Air Model for Chemical and Thermal Nonequilibrium Calculations to 30 000 K, NASA Reference Publication RF-1232, 1990.

References: 1- Sagnier, Ph., Joly, V, and Marmignon, C., “Analysis of Nonequilibrium Flow Calculations and Experimental Results Around a Hyperboloid-flare Configuration”, 2nd European Symposium on Aerodynamics for Space Vehicles, 1995.

2- Kurbatskii, K.A, Kumar, R., and Mann, D., “Simulation of External Hypersonic Problems Using Fluent 6.3 Density-Based Coupled Solver”, 2nd European Conference for Aerospace Sciences

Flow Over Hyperboloid Flare

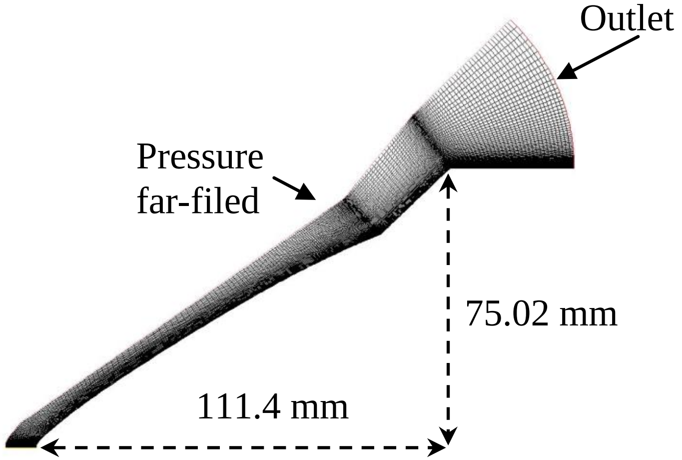

M = 15
P_s = 300 Pa
T_s = 514 K
M_{N2} =0.78
M_{O2}=0.22

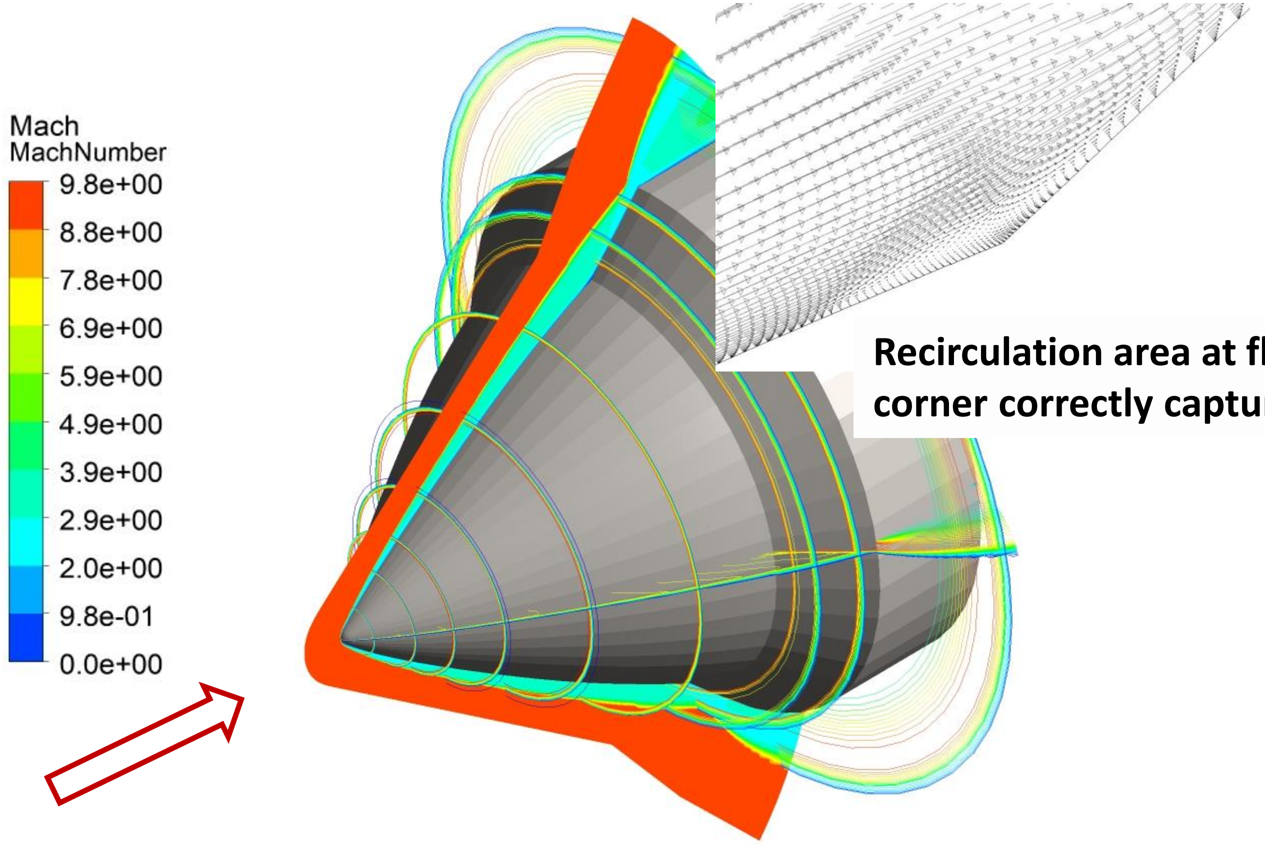

Recirculation area at flap corner correctly captured

Flow Over Hyperboloid Flare: validation of fluid solution

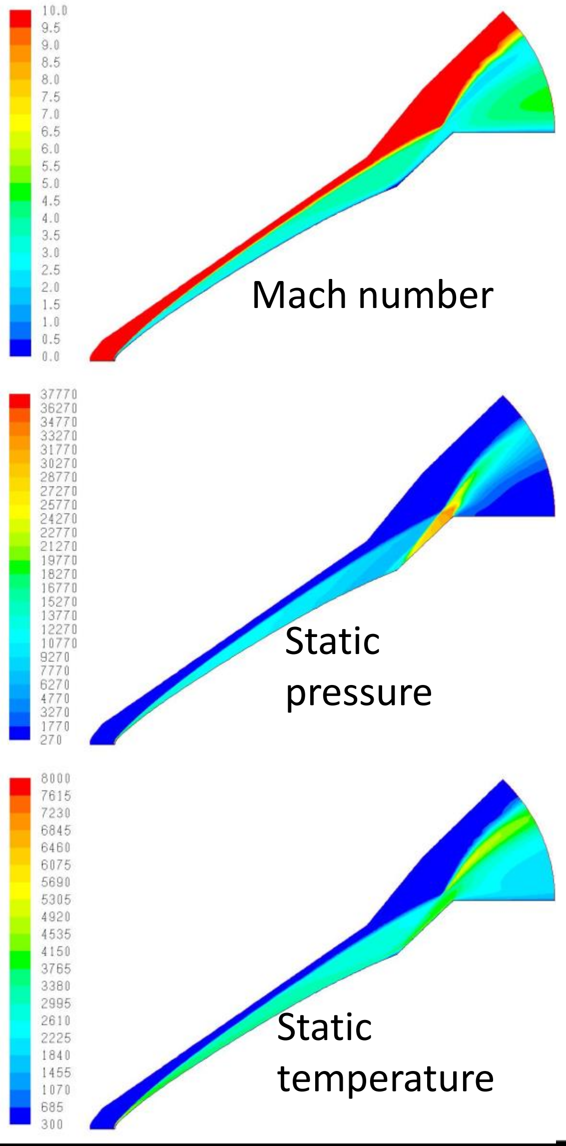

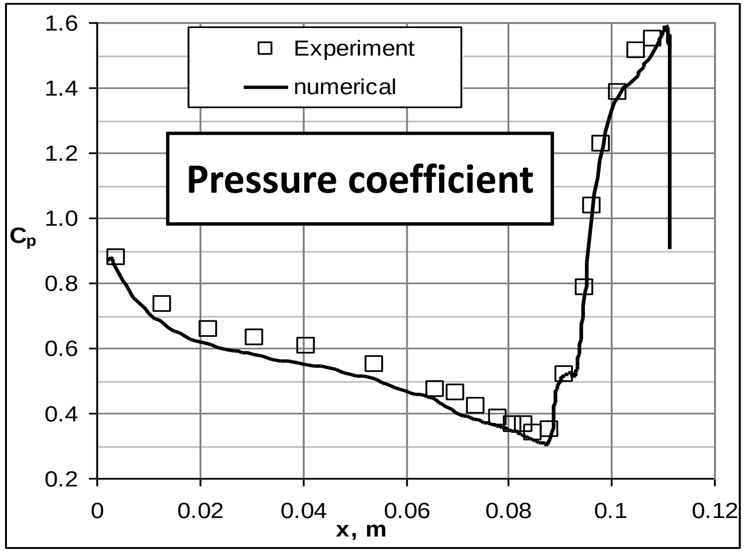

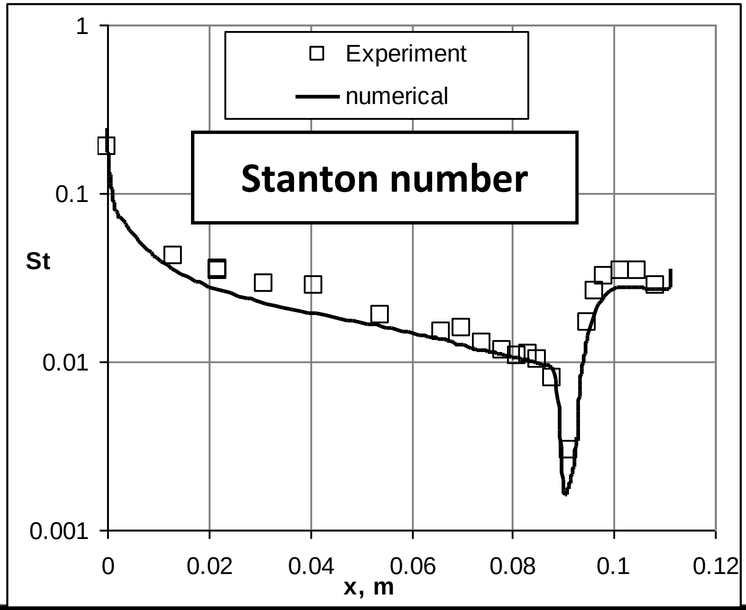

* Validation performed at Mach 10

Ansys

Plasma Inclusion in Ansys HFSS

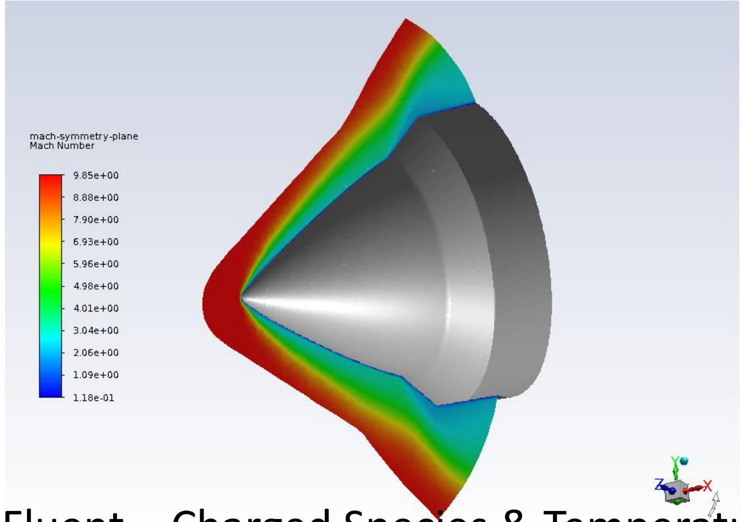

Fluent – Charged Species & Temperature

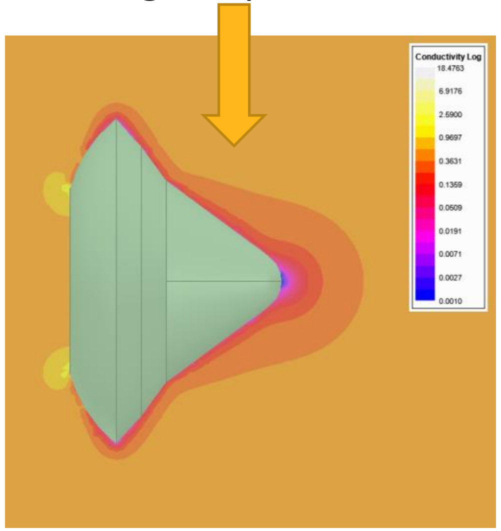

Map to Spatially Varying Conductivity

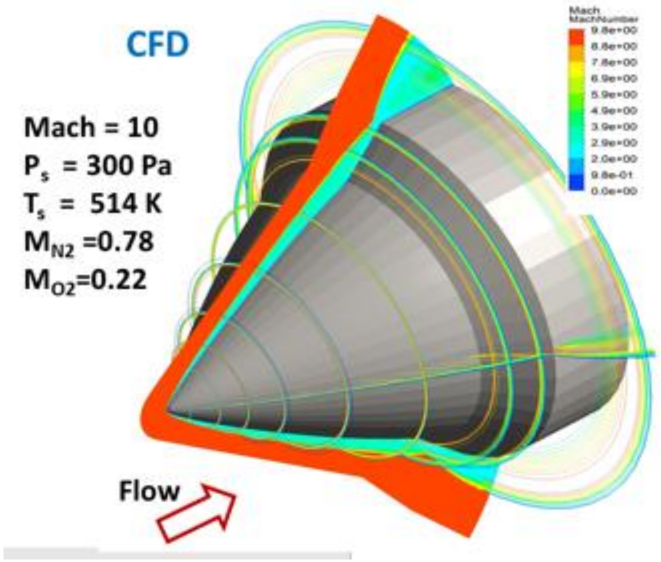

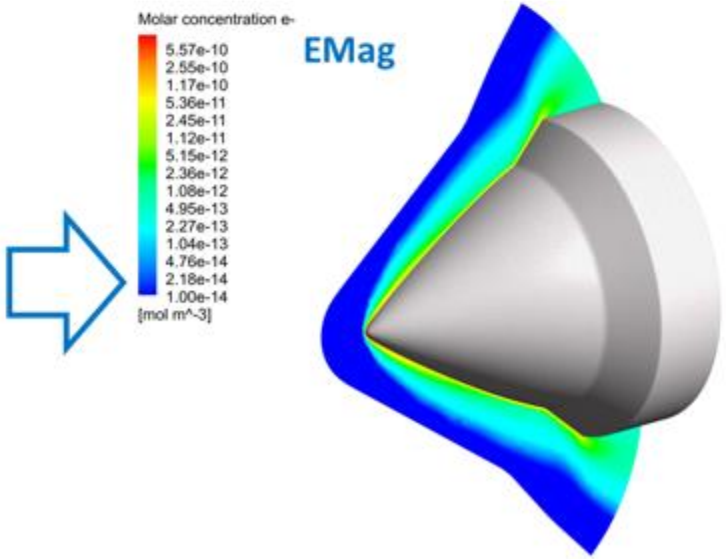

Ion concentration around the vehicle

Antenna Simulation Comparison

- Helical antenna at 1GHz
  - Impedance Z_ant = 3.7 + i*218.65

Freq [GHz]	dB(St(Helix1_T1,Helix1_T1)) Setup1 : LastAdaptive	re(Zt(Helix1_T1,Helix1_T1)) Setup1 : LastAdaptive	im(Zt(Helix1_T1,Helix1_T1)) Setup1 : LastAdaptive
1.000000	-66.247662	3.702541	218.647442

Antenna in Air

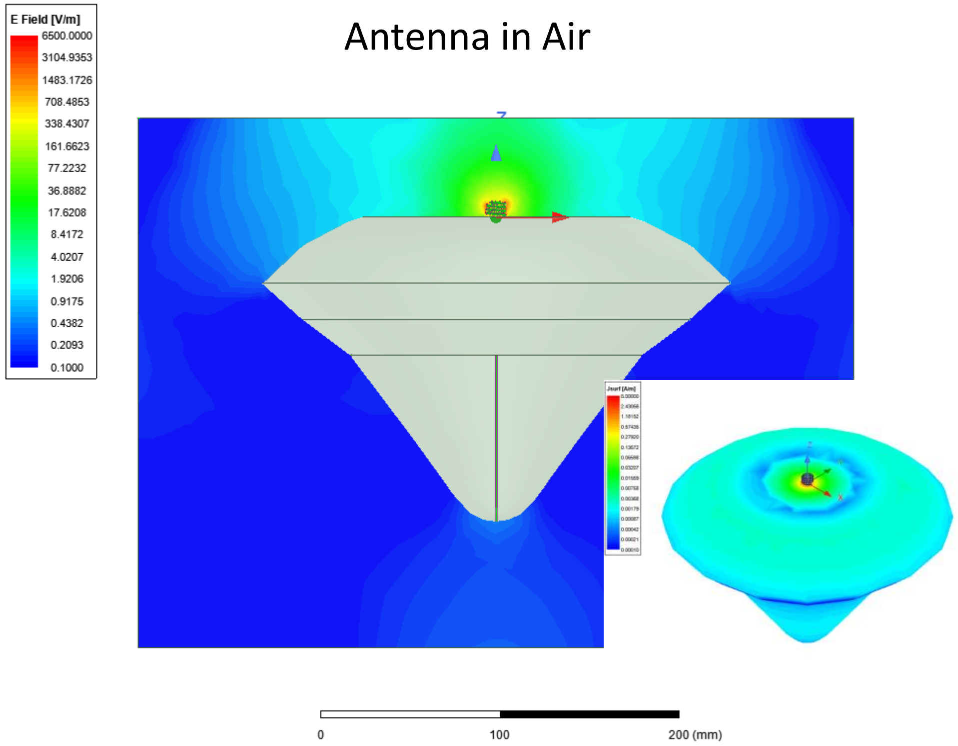

Mapped Complex Conductivity

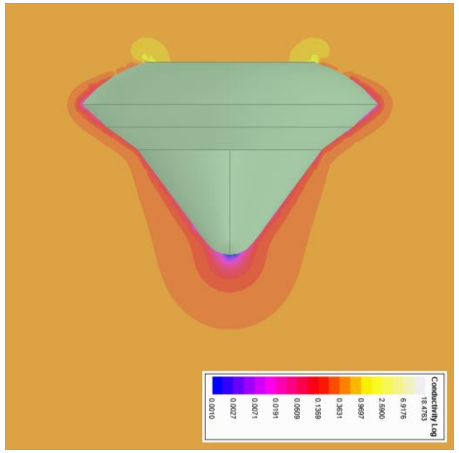

Freq [GHz]	dB(St(Helix1_T1,Helix1_T1)) Setup1 : LastAdaptive	re(Zt(Helix1_T1,Helix1_T1)) Setup1 : LastAdaptive	im(Zt(Helix1_T1,Helix1_T1)) Setup1 : LastAdaptive
1.000000	-0.003267	2.043576	18.170713

Antenna in Ionized Air

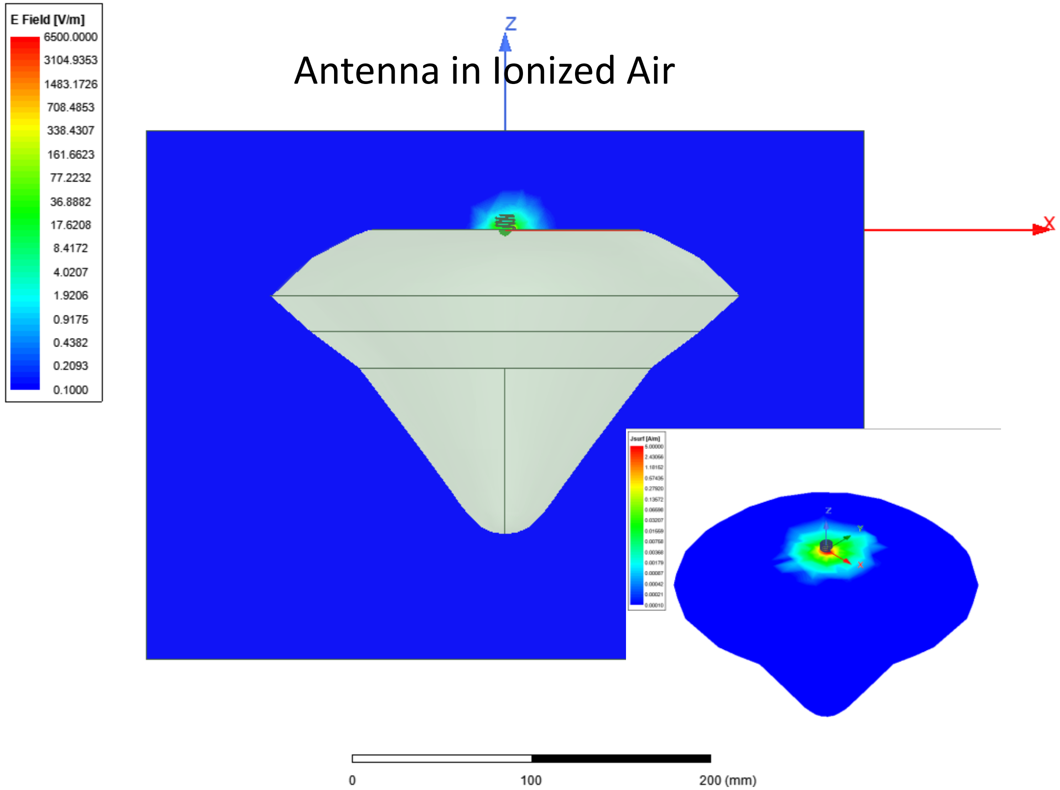

Ansys Technology Stack for Hypersonics

Aerodynamics | **Propulsion** | **Materials & Structures** | **Communication & Tracking** | **System Integration**

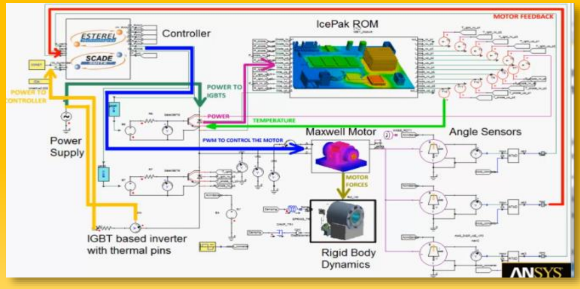

Control system/ sensors on Vehicle

- Simulate flight controls using physical behavior of vehicle
  - ✓ Vary environmental conditions
  - ✓ Vary trajectories
- System compatibility

Sensor fusion & actuation

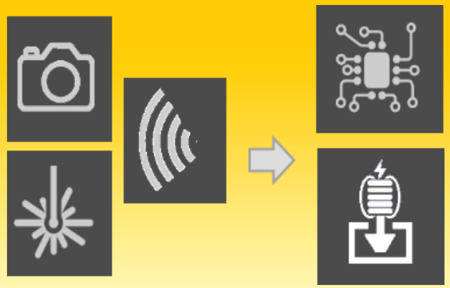

- Raw data or object level fusion
- Closed-loop verification

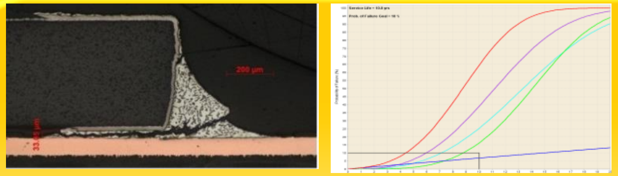

Electronics reliability

- High-temperature material degradation
- Integrated circuit wear-out
- Life testing
- Thermal fatigue

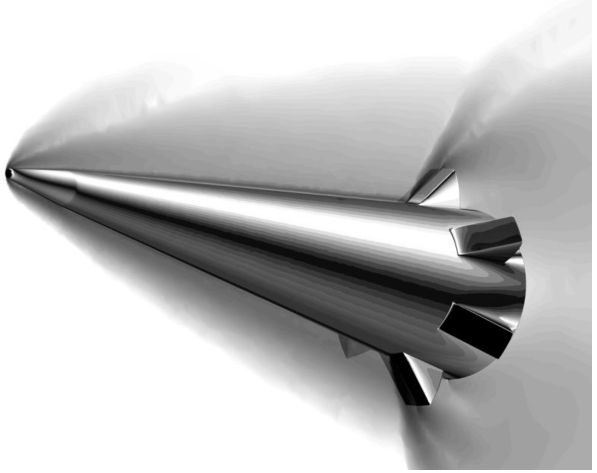

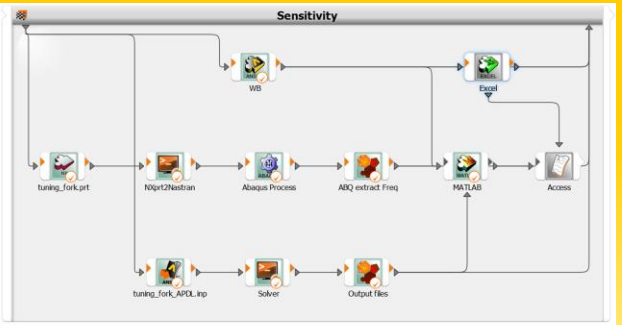

Open Simulation Platform

- Connect Ansys simulations using APIs to:
  - ✓ In-house codes and
  - ✓ 3rd party tools
- Phoenix integration

Navigation, guidance, and control

- MBSE for controls development
- Virtual environment for testing

Ansys Technology Stack for Hypersonics

Aerodynamic

& Tracking

System Integration

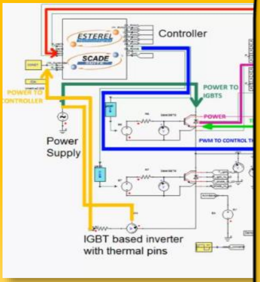

Control system/ s

- Simulate flight con vehicle
  - ✓ Vary enviror
  - ✓ Vary traject
- System compatibili

Sensor fusio

- Raw data or object level fusion
- Closed-loop verification

Military Wargame

- Integrate realistic 3D physical models in simulated interconnected environment
- Ansys AGI solutions simulate realistic physics-based system behavior

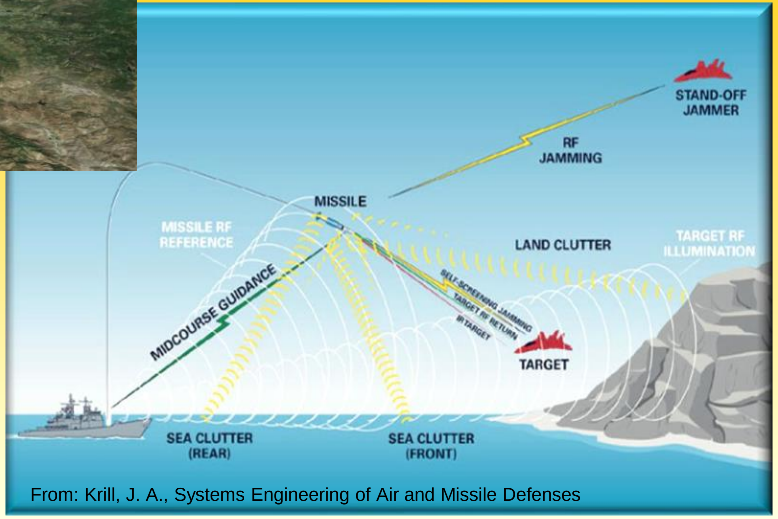

From: Krill, J. A., Systems Engineering of Air and Missile Defenses

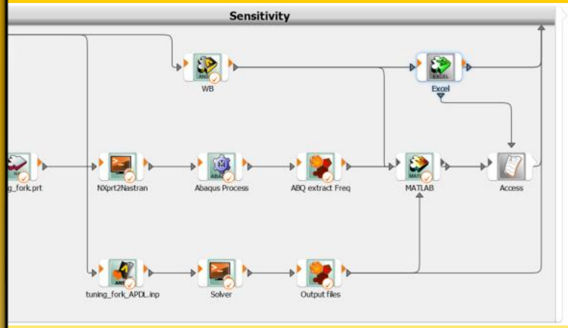

n Simulation Platform

- nnect Ansys simulations using APIs to:
  - ✓ In-house codes and
  - ✓ 3rd party tools
- penix integration

avigation, guidance, and control

- MBSE for controls development
- Virtual environment for testing

Mission Modeling with Ansys AGI

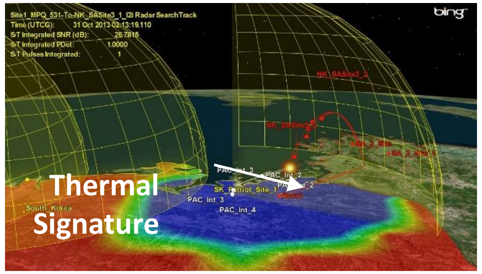

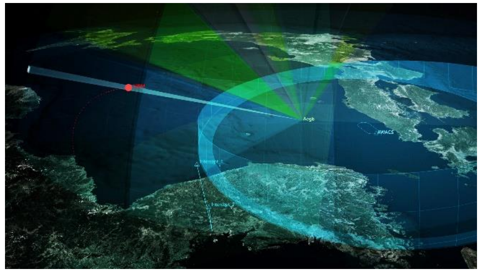

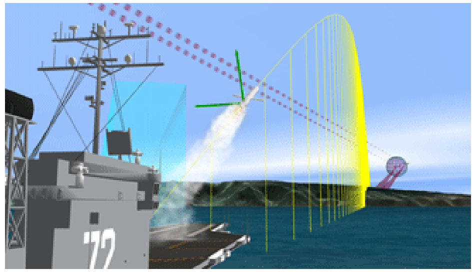

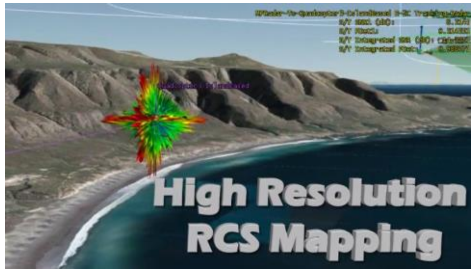

AGI
An Ansys Company

Trajectory Data

- Time
- Altitude
- Mach Number
- Angle of Attack

Aviator Performance Model
EO/IR Target Signature

Dynamic pointing geometries

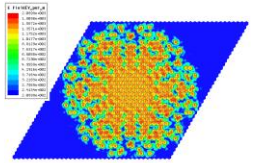

RCS / Antenna Gain

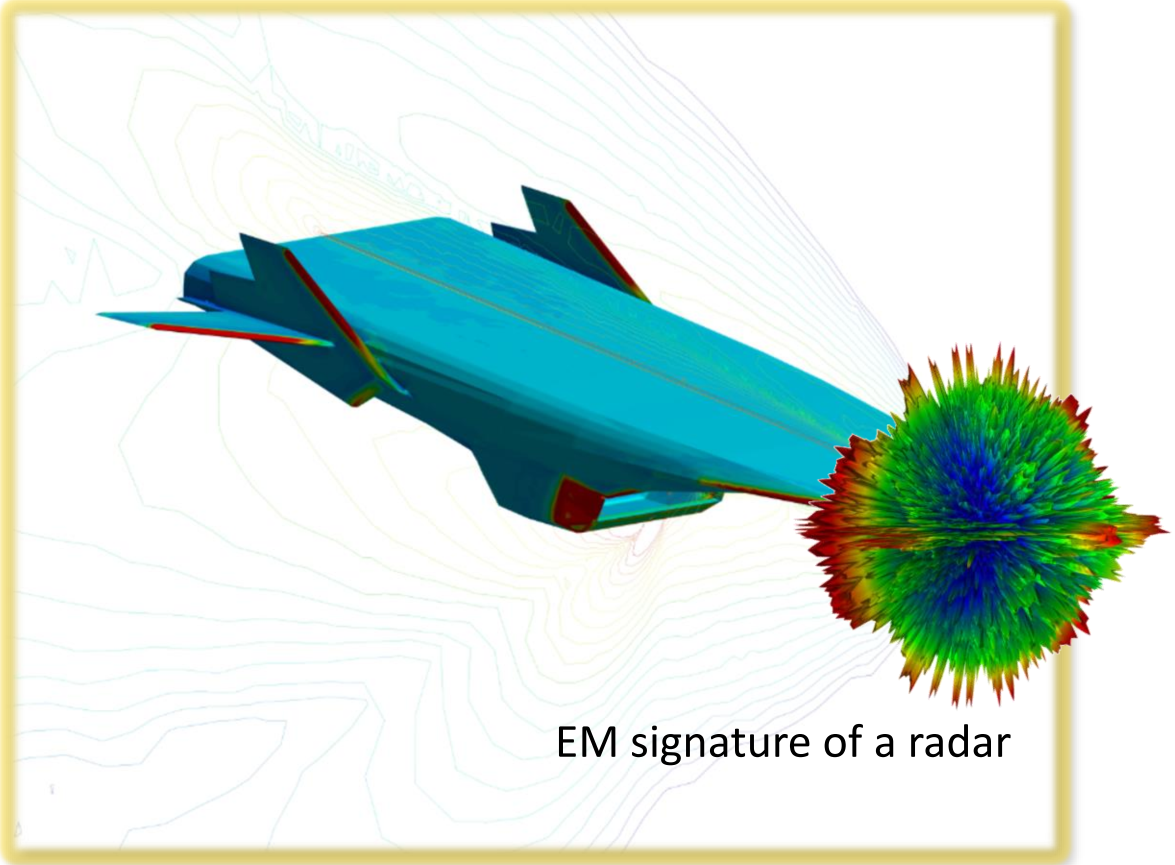

https://www.ansys.com/blog/acquisition-of-agi-extends-the-digital-thread

New Ansys R&D collaborations in hypersonics

- **University of Texas, Arlington**
  - Aerodynamic Research Lab (ARC): Director Prof Maddalena
  - The only US academic institution with arc-jet facility.
  - Inaugurated in summer 2019, with $1.5M funding from US Navy/DARPA
  - Cutting-edge experimental research in hypersonics (aerothermodynamics, SCRAMJET propulsion, ablation)
  - Currently worki

These universities are members of the
University Consortium for Applied Hypersonics (UCAH)

- **Missouri Scien**
  - Aerodynamic C
  - Research spons
    - Simulation te
    - Effect of particles on high-speed vehicles
    - Uncertainty Quantification
  - ARL has recently won an NSF grant for ~$2M to deploy a supercomputer dedicated to computer simulations.

- **University of Colorado, Boulder**
  - Collaboration with UC Boulder's Non-Equilibrium Gas and Plasma Dynamics Lab on hybrid coupling of CFD and DSMC methods for rarefied flows.

Accelerate Development to Counter a Hypersonic Threat with Ansys

- ✓ Uniquely poised to address the needs for developing the next generation Hypersonic vehicles.
- ✓ Open platform to integrate existing and future digital efforts
- ✓ Expansive Portfolio of Multiphysics Tools
  - ✓ Rapid Design
  - ✓ High Fidelity Component Modeling
  - ✓ System Modeling
  - ✓ Physics based Multidomain Modeling
  - ✓ Component to Mission Engineering
- ✓ Bridging gaps through strategic Partnerships

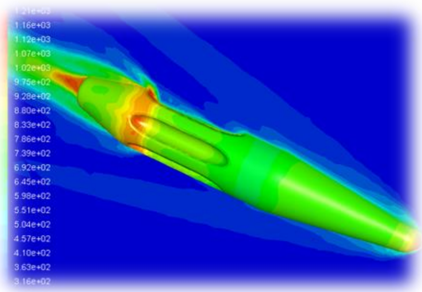

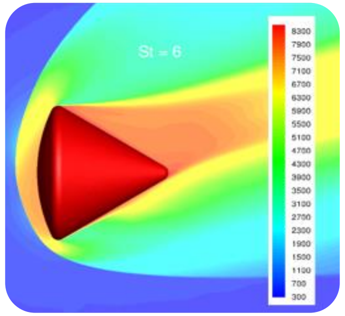

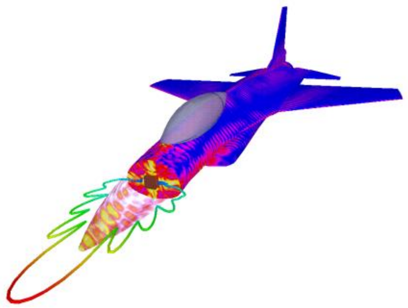

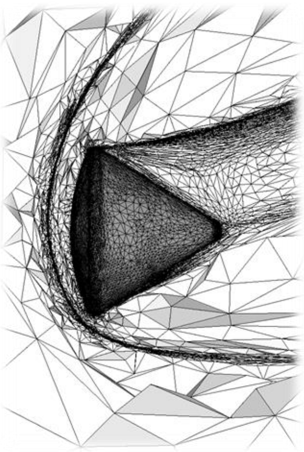

Extensive suite of validations for hypersonic flows

case	flow regime	Mach No.	AoA	geometry	image	Publication	Exp Reference
T-1	Transonic	0.6 to 0.8	Range from -5 to +2	DLR-F6 wing-body and wing-body-nacelle-pylon	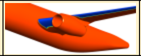	Eisenhut, S. & Frank, T. 2nd AIAA Drag Prediction Workshop, DLR-F6 Aircraft Model, WB and WBNP Configuration, Orlando, FL, June 21-22, 2003.	2nd AIAA CFD Drag Prediction Workshop
T-2	Transonic	0.85	2.5 to 2.7	CRM wing-body and wingbody-nacelle-pylon	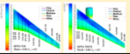	Zore, K., Sasanapuri, B., Shah, S., Bish, E., & Sotkes, J. ANSYS Simulation Results for the 6th AIAA Drag Prediction Workshop, Washington , DC, June 16-17, 2016.	6th AIAA CFD Drag Prediction Workshop
T-3	Transonic	0.85	-	Transonic Cavity Noise	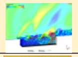	Kurtabatskii, K., Menter, F., Schuetze, J., & Fujii, A. Numerical Simulation of Transonic Cavity Noise using Scale-Adaptive Simulation (SAS) Turbulence Model, Internoise 2011, Osaka, Japan, September 4-7, 2011.	M. J. Henshaw, "M219 Cavity Case," Verification and Validation Data for Computational Unsteady Aerodynamics, Tech. Rep. RTO-TR-26, AC/323(AVT)TP/19 (2000).
T-4	Transonic	0.4, 0.8, 0.9	2	RAE wing body		Ansys internal validation	Treadgold, D., Jones, A., and Wilson, K., "Pressure Distribution Measured in the RAE 8ft x 6ft Transonic Wind Tunnel on RAE Wing 'A' in Combination with an Axi-Symmetric Body at Mach Numbers of 0.4, 0.8 and 0.9," AGARD-AR-138, Appendix B4.
T-5	Transonic	0.95, 1.2	0	store drop - delta wing		Snyder, D.O., Koutsavdis, E.K., Anttonen, J.S.R.: "Transonic store separation using unstructured CFD with dynamic meshing", Technical Report AIAA-2003-3913, 33th AIAA Fluid Dynamics Conference and Exhibition, American Institute of Aeronautics and Astronautics, 2003.	Heim, E. : "CFD wing/pylon/finned store mutual interference wind tunnel experiment", DTIC Document, (1991).
Sup-1	Supersonic	1.2	165, 180	Apollo capsule	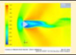	Ansys internal validation	Moseley, W. Graham, R., & Hughes, J., Aerodynamic Stability Characteristics of the Apollo Command Module, NASA-TN D-4688, August 1968.
Sup-2	Supersonic	3.48	0	re-entry capsule w/ counter-flowing jet		Ansys internal validation	Daso, O. E. et. al., " Dynamics of Shock Dispersion and Interactions in Supersonic Freestreams with Counterflowing Jets," AIAA Journal, Vol. 47, No. 6, June 2009.
Sup-3	Supersonic	2.5,3.5	Range from -5 to +18	tandem canard missile	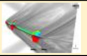	Rao, V., Viti, V., & Abanto, J. CFD simulations of super/hypersonic missiles: validation, sensitivity analysis, and improved design, AIAA SciTech Forum, 6-10 January 2020, Orlando, FL, January 2020.	Blair, Jr., A. B., Allen, J. M., Hernandez, G., Effect of tail-fin span on stability and control characteristics of a canardcontrolled missile at supersonic Mach number, NASA Technical Paper 2157, June 1983.
Sup-4	Supersonic	2.4	-	SCRAMJET supersonic combustion	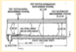	Ansys internal validation	Burrows, M. C. and Kurkov, A. P., "Analytical and Experimental Study of Supersonic Combustion of Hydrogen in a Vitiated Airstream," NASA-TM-X-2828, Sep. 1973.
Hyp-01	Hypersonic	6	0,10	Aerospike	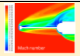	Rao, V., Viti, V., & Abanto, J. CFD simulations of super/hypersonic missiles: validation, sensitivity analysis, and improved design, AIAA SciTech Forum, 6-10 January 2020, Orlando, FL, January 2020.	Huebner, L., et al., Experimental results on the feasibility of an aerospike for hypersonic missiles, 33rd Aerospace Sciences Meeting and Exhibit, Aerospace Sciences Meetings, Reno, NV, 1995.
Hyp-02	Hypersonic	6.5	-	Hypersonic SCRAMJET	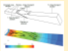	Babu, V., Run Like the Wind, ANSYS Advantage, Volume VIII, Issue 1, 2014.	Kumaran, K. & Babu, V., Mixing and combustion characteristics of kerosene in a model supersonic combustor, Journal of Propulsion and Power 25 (3), 583-592.
Hyp-03	Hypersonic	7.93	0	Hypersonic flow over Mars Pathfinder (70 degree sphere cone)		Ansys internal validation	Paterna, D., Monti, R., Savino, R., & Esposito, A., Experimental and Numerical Investigation of Martian Atmosphere Entry, Journal of Spacecraft and Rockets, Vol. 39, No. 2, March-April 2002.
Hyp-04	Hypersonic	8.3	-	Hypersonic double fin inlet		upcoming AIAA paper Viti, V., Crawford, B., Arguinzoni, C., Rao, V., & Zori, L. Numerical simulations of four hypersonic vehicles using a density-based CFD solver: validation, analysis and sensitivity to material properties 2020.	Kussoy, M.I., Horstman, K. C., Horstman, C. C., Hypersonic Crossing Shock-Wave/Turbulent Boundary-Layer Interactions, AIAA Journal 31 No. 12, 2197-2203, 1993
Hyp-05	Hypersonic	10	0	Hyperboloid Flare		Kurbatskii, K.A, Kumar, R., and Mann, D., "Simulation of External Hypersonic Problems Using Fluent 6.3 Density-Based Coupled Solver", 2nd European Conference for Aerospace Sciences	Sagnier, Ph., Joly, V, and Marmignon, C., "Analysis of Nonequilibrium Flow Calculations and Experimental Results Around a Hyperboloid-flare Configuration", 2nd European Symposium on Aerodynamics for Space Vehicles, 1995.
Hyp-06	Hypersonic	10.3		Biconic Reentry Vehicle with Six Extended Flaps	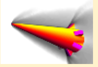	upcoming AIAA paper Viti, V., Crawford, B., Arguinzoni, C., Rao, V., & Zori, L. Numerical simulations of four hypersonic vehicles using a density-based CFD solver: validation, analysis and sensitivity to material properties 2020.	Jordan, T.M., Buffington, R.J., Aerodynamic Model for a Hemispherically-Capped Biconic Reentry Vehicle with Six Drag Flaps. AIAA Paper 87-2364, 1987.
Hyp-07	Hypersonic	12.6	0	sharp-nosed double cone	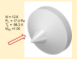	upcoming AIAA paper Viti, V., Crawford, B., Arguinzoni, C., Rao, V., & Zori, L. Numerical simulations of four hypersonic vehicles using a density-based CFD solver: validation, analysis and sensitivity to material properties 2020.	Effect of Vibrational Non-Equilibrium on Hypersonic Double-Cone Experiments Ioannis Nompelis and Graham V. Candler (AIAA Journal Vol.41, No.11, Nov 2003
Hyp-08	Hypersonic	19.4	0	FIRE II re-entry vehicle	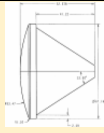	upcoming AIAA paper Viti, V., Crawford, B., Arguinzoni, C., Rao, V., & Zori, L. Numerical simulations of four hypersonic vehicles using a density-based CFD solver: validation, analysis and sensitivity to material properties 2020.	Hash, D., Olejniczak, J., Wright, M., Prabhu, D., Pulsonetti, M., Hollis, B., Gnoffo, P., Barnhardt, M., Nompelis, I., FIRE II Calculations for Hypersonic Nonequilibrium Aerothermodynamics Code Verification: DPLR, LAURA,and US3D, 45th AIAA Aerospace Sciences Meeting and Exhibit, Reno, NV, AIAA Paper 2007-605, January 2007. Wright, M., Loomis, M., Papadopoulos, P., Aerothermal Analysis of the Project Fire II Afterbody Flow, Journal of Thermophysics and Heat Transfer, vol. 17 No.2, April-June 2003.
Hyp-09	Hypersonic	25	0	blunt axisymmetric sphere-cone	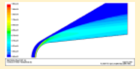	Ansys internal validation	Lee, K. & Gupta, R. , Viscous-Shock-Layer Analysis of Hypersonic Flows over Long Slender Vehicles, NASA Contractor Report 189614 March 1992.
Hyp-10	Hypersonic	29	0	sphere		Kurbatskii, K.A, Kumar, R., and Mann, D., "Simulation of External Hypersonic Problems Using FLUENT 6.3 Density-Based Coupled Solver", 2nd European Conference for Aerospace Sciences.	Widhopf, G. F., and Wang, J. C. T., "A TVD Finite-Volume Technique for Nonequilibrium Chemically Reacting Flows", AIAA Paper 1988-2711 Dellinger, T. C., "Computation of Nonequilibrium Merged Stagnation Shock Layers by Successive Accelerated Replacement", AIAA Journal, 9(2):262-269, 1971.
Hyp-11	Hypersonic	10.6, 11.1	0	Hypersonic transition on a Flat Plate	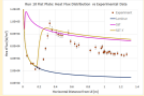	Aliaga, C., Guan, K., Selvanayagam, J., Sokes, J., Viti, V., & Menter, F. Hypersonic Applications of the Laminar-Turbulent Transition SST Model in ANSYS Fluent AIAA Hypersonic Transition Paper to be published in 2020.	Holden, M., MacLean, M., Wadhams, T., and Mundy, E., "Experimental Studies of Shock Wave/Turbulent Boundary Layer Interaction in High Reynolds Number Supersonic and Hypersonic Flows to Evaluate the Performance of CFD Codes", AIAA 2010-4468, 40th Fluid Dynamics Conference and Exhibit, Chicago, Illinois, June 28, 2010. Marvin, J.G., Brown, J.L., and Gnoffo, P.A., "Experimental Database with Baseline CFD Solutions: 2-D and Axisymmetric Hypersonic Shock-Wave/Turbulent-Boundary-Layer Interactions", NASA/TM-2013-216604, NASA: Ames Research Center, Moffett Field, CA, November 2013.
Hyp-12	Hypersonic	7.19	0	2d axisymmetric Hypersonic transition on a Blunt Cone Cylinder Flare junction	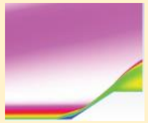	same as above	MacLean, M., Wadhams, T., Holden, M., and Johnson, H., "A Computational Analysis of Ground Test Studies of HIFiRE-1 Transition Experiment," AIAA 2008-641, 46th AIAA Aerospace Sciences Meeting and Exhibit, Reno, Nevada, January 7, 2008. Wadhams, T., Mundy, E., MacLean, M., and Holden, M., "Pre-Flight Ground Testing of the Full-Scale HIFiRE-1 Vehicle at Fully Duplicated Flight Conditions: Part II, AIAA 2008-639, 46th AIAA Aerospace Sciences Meeting and Exhibit, Reno, Nevada, January 7, 2008.
Hyp-13	Hypersonic	7.16	0	2d axisymmetric Hypersonic transition on a Sharp Cone Cylinder Flare junction	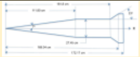	same as above	same as above
Hyp-14	Hypersonic	7.19	0	3d Hypersonic transition on a Blunt Cone Cylinder Flare junction		same as above	same as above
Hyp-15	Hypersonic	Vel ~ 7.8 km/s		RF Blackout during Space Probe Reentry	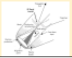	validation work-in-progress	Bendoukha, S., Okuyama, K., & Szasz, B. A Study of Radio Frequency Blackout for Space Probe During Atmospheric Reentry Phase, International Journal of Research Granthaalayah, Vol. 5 (Iss. 3): March, 2017.

We are always looking for good quality wind tunnel data and physical test data for benchmarking our solvers

Ansys CFD Hypersonics Training

Improve engineering productivity using advanced engineering simulation

Contact: Rodger.Zhao@ansys.com

Learn how to use Ansys CFD to design and analyze hypersonic systems

- 2-day on-site course (1-week mentoring project total)
- Combination of lectures and hands-on workshops
- Work on your own problem on the second day
- Maximum 10 students per class

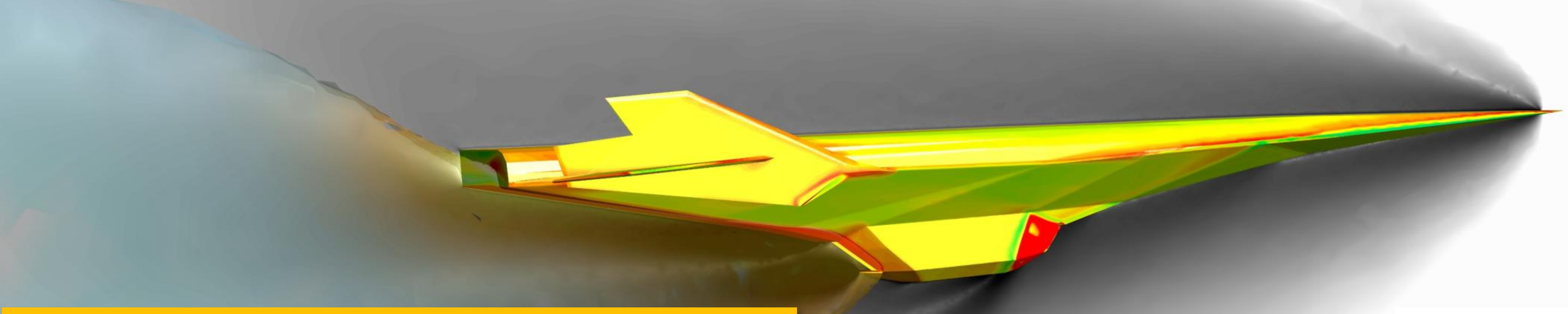

Extending training material to include **structural** and **electromagnetic** modules

What you will learn

- The value of simulation for hypersonic systems
- Using Ansys CFD for hypersonic vehicles
- Modeling advanced physical processes including chemical non-equilibrium
- Simulation strategies to improve productivity

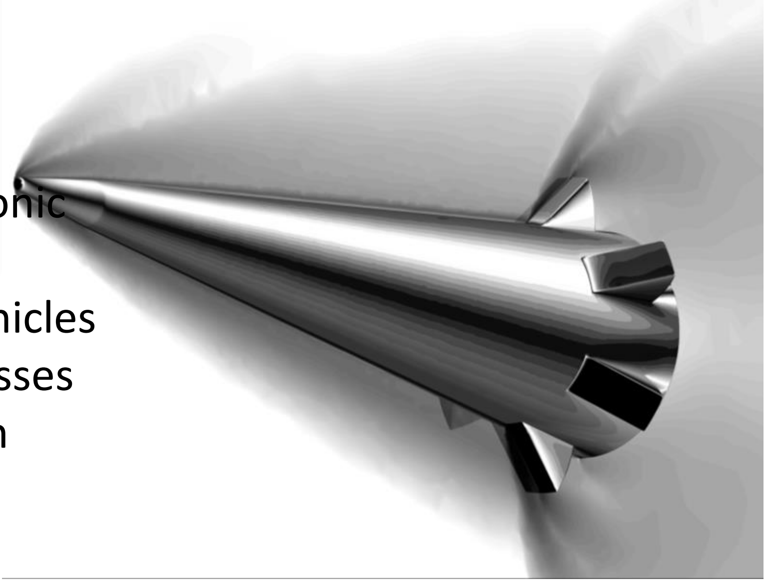

Selected Ansys publications on hypersonics

- Viti, V., Rao, V., Crawford, B., Arguinzoni, C, Zori, L., “Numerical simulations of four canonical hypersonic vehicles and test cases", AIAA 2020-2723, AIAA Aviation 2020, Nashville, TN, June, 2020.
- Aliaga, C., Guan, K., Selvanayagam, J., Stokes, J., Viti, V., Menter, F., Hypersonic Applications of the Laminar-Turbulent Transition SST Model in ANSYS Fluent, AIAA Hypersonics 2020, Montreal, QC, Canada, March 2020.
- Tiliakos, N., DeSorbo, J., Martin, N., Viti, V., Laurence, S., Rabin, O., “A Roadmap for Obtaining and Implementing Heat Flux Measurements in the Hypersonic Environment”, AIAA Hypersonics 2020, Montreal, QC, Canada, March 2020.
- Rao, V., Viti, V., Abanto, J., “CFD simulations of super/hypersonic missiles: validation, sensitivity analysis and improved design", AIAA 2020-2123, AIAA ScitTech 2020, Orlando, FL, January 6-10th, 2020.
- Kumar, A., Kumar, V., Nakod, P., Rajan, A., Schütze, J., Multiscale Modelling of a Doublet Injector Using Hybrid VOF-DPM Method, AIAA 2020-2284, AIAA ScitTech 2020, Orlando, FL, January 6-10th, 2020.
- Viti, V., Svihla, K., Marinus, S., Dodd, E., Tharp, J., Crawford, B., Miller, C., Staggs, E., “Development and validation the ANSYS hypersonic prototype”, Hypersonic Technology and Systems Conference, Alexandria, VA, 26-29 August, 2019.
- Babu, V., Flight like the wind, ANSYS Advantage, Vol.8, 2014.
- Ground, C., Vergine, F., Maddalena, L., Viti, V., “Flow characteristics of a strut injector for scramjets: numerical and experimental analysis", TFAWS2014-I-02, NASA Thermo and Fluids Analysis Workshop, Cleveland, OH, August 4-8th, 2014.
- Ground, C., Vergine, F., Maddalena, L., Viti, V., “Experimental and numerical investigation of the flow characteristics of a strut injector for scramjets”, AIAA 2014-3217, 19th AIAA International Space Planes and Hypersonic Systems and Technologies Conference, Atlanta, GA, 16-20 June, 2014.
- Kurbatskii, K., Montanari, F., Application of Pressure-Based Coupled Solver to the Problem of Hypersonic Missiles with Aerospikes, 45th AIAA Aerospace Sciences Meeting and Exhibit 8 - 11 January 2007, Reno, Nevada, AIAA Paper 2007-462.
- Kurbatskii, K., Kumar, R., Mann, D., Simulation of External Hypersonic Problems Using FLUENT 6.3 Density-Based Coupled Solver, 2ND EUROPEAN CONFERENCE FOR AEROSPACE SCIENCES EUCASS, Brussell, Belgium, 1-6 June 2007.
- Paterna, D., Monti, R., Savino, R., Esposito, A., “Experimental and numerical investigation of Martian atmosphere entry”. Journal of spacecraft and rockets, Vol. 39, No.2, March-April 2002.
- Savino, R., De Stefano Fumo,M., Paterna, D., Serpico, M., Aerothermodynamic study of UHTC-based thermal protection systems, Aerospace Science and Technology, Volume 9, Issue 2, pp.151-160, March 2005.
- Savino,R., Paterna,D.,Blunted cone–flare in hypersonic flow, Computers & Fluids, Volume 34, Issue 7, pp. 859-875, August 2005.

Thank you

Swati Saxena
swati.saxena@ansys.com

Find out more about Ansys hypersonics solutions:
https://www.ansys.com/products/fluids/hypersonic-speed
https://www.ansys.com/resource-library/webinar/challenges-hypersonic-vehicle-design